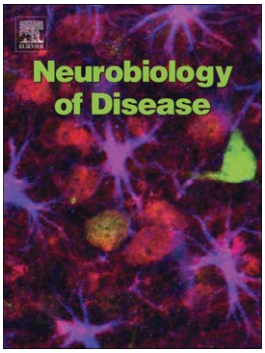

Effects of L-dopa priming on cortical high beta and high gamma oscillatory activity in a rodent model of Parkinson's disease

Kristin B. Dupre, Ana V. Cruz, Alex J. McCoy, Claire Delaville, Colin M. Gerber, Katherine W. Eyring, Judith R. Walters

PII: S0969-9961(15)30088-7
DOI: doi: 10.1016/j.nbd.2015.11.009
Reference: YNBDI 3634

To appear in: *Neurobiology of Disease*

Received date: 17 June 2015
Revised date: 6 November 2015
Accepted date: 11 November 2015

Please cite this article as: Dupre, Kristin B., Cruz, Ana V., McCoy, Alex J., Delaville, Claire, Gerber, Colin M., Eyring, Katherine W., Walters, Judith R., Effects of L-dopa priming on cortical high beta and high gamma oscillatory activity in a rodent model of Parkinson's disease, *Neurobiology of Disease* (2015), doi: 10.1016/j.nbd.2015.11.009

Effects of L-dopa priming on cortical high beta and high gamma oscillatory activity in a rodent model of Parkinson's disease

Running Title: Cortical high gamma during dyskinesia

Kristin B. Dupre[1], Ana V. Cruz[1], Alex J. McCoy[1], Claire Delaville[1], Colin M. Gerber[1], Katherine W. Eyring[1], and Judith R. Walters[1]

[1]Neurophysiological Pharmacology Section, National Institute of Neurological Disorders and Stroke, National Institutes of Health, Bethesda, MD 20892-3702

Corresponding Author:
Judith R. Walters, Ph.D.
Neurophysiological Pharmacology Section
National Institute of Neurological Disorders and Stroke
National Institutes of Health
35 Convent Drive
Building 35, Room 1C905
Bethesda, MD 20892-3702
Phone: 301-496-2067
Fax: 301-402-0625
E-mail: waltersj@ninds.nih.gov

Abstract length: 1,917 (characters w/ spaces)
Number of pages: 40
Number of tables: 1
Number of figures: 6
Number of words (manuscript body): 8765
Abstract: 276
Introduction: 555
Discussion: 1895

A**bbreviations:** 5-HT, serotonin; 6-OHDA, 6-hydroxydopamine; 8-OH-DPAT, (+)-8-Hydroxy-2-(dipropylamino)tetralin hydrobromide; AIMs, abnormal involuntary movements; ALO, axial, limb, and orolingual; benserazide, DL-serine 2-(2,3,4-trihydroxybenzyl) hydrazide hydrochloride; Aq, aqueduct (Sylvius); DA, dopamine; DPAT, 8-OH-DPAT; FFT, fast Fourier-transform; FTG, finely-tuned gamma; GPi, globus pallidus internal segment; i.p., intraperitoneally; L-dopa, levodopa; LFP, local field potential; PCA, principal component analysis; PING, pyramidal-interneuronal gamma; PD, Parkinson's disease; quinpirole, (-)-Quinpirole hydrochloride; RM, repeated-measures; RMS, root mean square; SKF81297, R(+)-SKF-81297 hydrobromide; SN, substantia nigra; SNR, signal-to-noise ratio; STN, subthalamic nucleus; STWA, spike-triggered waveform average; TH, tyrosine hydroxylase; WAY, WAY100635; WAY100635, N-[2-[4-(2-Methoxyphenyl)-1-piperazinyl]ethyl]-N-2-pyridinylcyclohexanecarboxamide maleate salt

Abstract

Prolonged L-dopa treatment in Parkinson's disease (PD) often leads to the expression of abnormal involuntary movements known as L-dopa-induced dyskinesia. Recently, dramatic 80 Hz oscillatory local field potential (LFP) activity within the primary motor cortex has been linked to dyskinetic symptoms in a rodent model of PD and attributed to stimulation of cortical dopamine D1 receptors. To characterize the relationship between high gamma (70-110 Hz) cortical activity and the development of L-dopa-induced dyskinesia, cortical LFP and spike signals were recorded in hemiparkinsonian rats treated with L-dopa for 7 days, and dyskinesia was quantified using the abnormal involuntary movements (AIMs) scale. The relationship between high gamma and dyskinesia was further probed by assessment of the effects of pharmacological agents known to induce or modulate dyskinesia expression. Findings demonstrate that AIMs and high gamma LFP power increase between days 1 and 7 of L-dopa priming. Notably, high beta (25-35 Hz) power associated with parkinsonian bradykinesia decreased as AIMs and high gamma LFP power increased during priming. After priming, rats were treated with the D1 agonist SKF81297 and the D2 agonist quinpirole. Both dopamine agonists independently induced AIMs and high gamma cortical activity that were similar to that induced by L-dopa, showing that this LFP activity is neither D1 nor D2 receptor specific. The serotonin 1A receptor agonist 8-OH-DPAT reduced L-dopa- and DA agonist-induced AIMs and high gamma power to varying degrees, while the serotonin 1A antagonist WAY100635 reversed these effects. Unexpectedly, as cortical high gamma power increased, phase locking of cortical pyramidal spiking to high gamma oscillations decreased, raising questions regarding the neural substrate(s) responsible for high gamma generation and the functional correlation between high gamma and dyskinesia.

Highlights:

- L-dopa reduces cortical high beta LFP activity while inducing dyskinesia
- L-dopa elicits the co-emergence of cortical high gamma LFP activity and dyskinesia
- D1 and D2 agonists individually induce cortical high gamma and dyskinesia
- 5-HT1A agonist reduces dyskinesia and cortical high gamma but increases high beta
- Phase-locking of cortical spikes is negatively correlated with high gamma LFP

Keywords: abnormal involuntary movements; beta; dopamine; dyskinesia; gamma; L-dopa; local field potential; motor cortex; oscillations; Parkinson's disease

Conflict of interest: None

Support: This work was supported by the Intramural Research Program of the National Institute of Neurological Disorders and Stroke, National Institutes of Health (NIH).

Acknowledgements: This work was supported by the Intramural Research Program of the National Institute of Neurological Disorders and Stroke, National Institutes of Health (NIH). We thank Tom Talbot, Daryl Bandy, and Newlin Morgan in the section of Instrumentation, National Institute of Mental Health–National Institute of Neurological Disorders and Stroke for design and fabrication of the rotary treadmill.

Introduction

Parkinson's disease (PD) is a neurodegenerative disorder that is caused by the death of dopaminergic neurons in the basal ganglia. PD primarily affects the motor system, inducing rigidity, slowness of movement, tremors and lack of coordination. Development of these motor impairments has been associated with the emergence of synchronized and oscillatory activity in the beta frequency range (13-35 Hz) in the motor cortex and basal ganglia of PD patients[1-7] and hemiparkinsonian rats.[8-12] Increased oscillatory activity has also been observed at lower frequencies in parkinsonian primates.[13-17]

Early stage PD patients are often treated with dopamine (DA) receptor agonists; however, the anti-parkinsonian efficacy of these agonists is somewhat limited and most patients are ultimately treated with Levodopa (L-dopa), the precursor to DA. Unfortunately, prolonged L-dopa treatment often leads to the development of abnormal involuntary movements, otherwise known as L-dopa-induced dyskinesia.[18] Though DA agonists are less likely to induce this side effect,[19, 20] they can also elicit dyskinesia in PD patients[21, 22] and hemiparkinsonian rats.[23-25] While the causes of dyskinesia are not fully understood, several mechanisms appear to be involved in its expression, including increased corticostriatal extracellular glutamate levels, glutamate transporter expression, and glutamate receptor phosphorylation.[26-29] Other important processes contributing to dyskinesia involve supraphysiological increases in L-dopa-derived DA within the striatum via serotonergic raphe-striatal neurons,[30, 31] supersensitive striatal DA receptors,[32] and enhanced striatonigral direct pathway activity.[33-36]

Recordings from the motor cortex and basal ganglia of PD patients following L-dopa treatment have shown decreases in exaggerated beta oscillatory activity and pronounced increases in local field potential (LFP) oscillations in the high gamma range (>50 Hz).[37, 38] In particular, a narrow band with a peak between 60-90 Hz, referred to as "finely-tuned gamma

(FTG)," is often observed in PD patients in the "on" state following L-dopa therapy, and power in this frequency range increases with movement.[39] While the functional role of FTG is uncertain, Halje and colleagues (2012) have recently reported similar activity within the primary motor cortex and striatum of hemiparkinsonian rats during L-dopa-induced dyskinesia. Indeed, distinct ~80 Hz oscillatory activity in these brain regions was expressed concurrently with AIMs. Local D1 receptor antagonism in the motor cortex abolished both the 80 Hz activity and dyskinesia. Moreover, the spiking activity of these cortical neurons shifted from an entrainment to the theta range (4-12 Hz) to an entrainment to high gamma (75-90 Hz) during L-dopa-induced dyskinesia.[40]

Many questions remain regarding the functional consequences of this high gamma cortical activity in parkinsonian and dyskinetic states. To better understand this phenomenon in the rat model of dyskinesia, the present study investigated the relative time courses of the development of high gamma cortical oscillations and the emergence of dyskinetic behavior during L-dopa priming in rats with either partial or full unilateral DA lesions. The effects of L-dopa priming on cortical high beta (25-35 Hz) LFP activity were also characterized. DA D1 and D2 agonists and the serotonin (5-HT)1A receptor agonist 8-OH-DPAT were used to further explore the association between cortical high gamma activity and dyskinesia. Finally, the relationships between cortical high gamma LFP oscillations and cortical neuronal spiking during various behavioral states were determined. Collectively, findings show that cortical high gamma LFP activity is positively associated with dyskinesia; however, subtle variability in this positive relationship and the apparent decrease of synchronized cortical spiking suggest a potential dissociation, which remains to be further explored.

Materials and Methods

All experimental procedures were conducted in accordance with the NIH Guide for Care and Use of Laboratory Animals and approved by the NINDS Animal Care and Use Committee. Every effort was made to minimize the number of animals used and their discomfort.

Surgical procedures

Male Sprague-Dawley rats (250-300 g upon arrival; Taconic Farms, Hudson, NY, USA) were housed on a 12 h light/dark cycle. Rats were anesthetized with 75 mg/kg ketamine and 0.25 mg/kg dexmedetomidine intraperitoneally (i.p.) before surgery for implantation of chronic recording electrodes. The incision area was shaved and a long-acting local anesthetic (1% mepivacaine HCl solution) was injected along the intended incision lines. Ophthalmic ointment was applied to prevent corneal dehydration and lidocaine gel placed in the ear canals. Rats were placed in a stereotaxic frame (David Kopf Instruments) fitted with atraumatic ear bars with their skull leveled in the dorsal–ventral plane. A heating pad was used to maintain body temperature at ~37°C.

All rats had electrode bundles implanted unilaterally in the left motor cortex layers 5/6. Electrode bundles consisted of eight stainless steel 50 µm Teflon insulated microwires with an additional ninth wire (~1 mm scraped tip) that served as a local reference (NB Labs, Denison, TX). Bundles had diameters of ~350 µm and each microwire had an impedance of ~0.6 MΩ, measured in physiological saline at 135 Hz. Holes were drilled over the target coordinates for the motor cortex (anterior: +2.0 mm from bregma; lateral: +2.5 mm; ventral: -2.0 mm, from skull surface). Ground wires from each bundle were connected to a screw located above the cerebellum and served as the instrument ground.

Rats were either kept as intact controls (n=4) or received a local injection of 6-hydroxydopamine (6-OHDA) into the medial forebrain bundle to lesion DA cells in the substantia nigra pars compacta at the time the electrode bundles were implanted (n=13). To

protect noradrenergic neurons, 6-OHDA injection was preceded by administration of 15 mg/kg desmethylimipramine (i.p.). Standard stereotaxic procedures were used to target the left medial forebrain bundle (anterior: +4.4 mm from the lambdoid suture; lateral: +1.2 mm from the sagittal suture; ventral: -8.3 mm from the skull surface). Six micrograms of 6-OHDA hydrobromide in 3 µl of 0.9% saline with 0.01% ascorbic acid was infused via a 27-gauge stainless steel cannula into the medial forebrain bundle at a rate of 1 µl/min over 3 min via a syringe pump (Harvard Apparatus). The cannula remained at the target site for 3 min after the infusion was completed to prevent diffusion of the neurotoxin. Five min post-surgery and one time/day for 2 days post-surgery, rats received an injection of 0.15% of ketoprofen in 0.9% NaCl solution.

Behavior

Treadmill Walking. A circular treadmill was used during recordings to control the behavior of the rats when walking. Seven to 10 days before the surgical procedures, rats were trained 2 times/day on 3 different days to walk in both directions on the circular treadmill at a speed of 8 RPMs. The presence of a paddle in the circular treadmill cylinder encouraged the rats to walk continuously in each specified direction. Following surgery, rats were gradually re-exposed to the treadmill during the first week and examined for their ability to walk in both directions. After unilateral DA cell lesions, the hemiparkinsonian rats could make reasonable progress on the circular treadmill if they were oriented in the direction ipsiversive to the unilateral lesion, with their affected paws on the outside of the circular path. If they were oriented in the opposite direction, contraversive to the lesion, they had considerable difficulty walking, and generally froze or reared and tried to turn around. As previously reported, the speed and design were adjusted so that both intact control and lesioned rats were capable of performing on the treadmill.[9] Lesion efficacy was also assessed by the stepping

test (see below) once per week post-lesion. During each recording session, rats were videotaped to provide further confirmation of the level of motor activity.

Stepping Test. The stepping test was performed one time prior to surgery and once per week for 4 weeks following surgery in rats that received 6-OHDA-lesions of the medial forebrain bundle (see Fig 1A and 1C). The number of adjusting steps taken by the forepaw in order to compensate for lateral movement was counted to determine the effects of lesion on motor performance.[41] Rats were moved laterally across a table at a steady rate of 90 cm/10 s. The rear part of the torso and the hindlimbs were lifted from the table and one forepaw was held by the experimenter so as to bear weight on the other forepaw. Each stepping test consisted of six trials for each forepaw, alternating between directions both forehand (defined as compensating movement toward the body) and backhand (defined as compensating movement away from the body) on the table. Data was derived by summing steps (forehand and backhand) of the lesioned forelimb and dividing them by the sum of steps (forehand and backhand) of the intact forelimb and multiplying by 100. Lower percentage of intact scores indicates greater forelimb akinesia.

Abnormal Involuntary Movements (AIMs). Rats were monitored and scored for AIMs using a previously described procedure.[24] Following L-dopa or DA agonist treatment, rats were individually placed in plastic cylinders (26.8 cm diameter, 27.5 cm height) and assessed for exhibition of axial, limb, and orolingual (ALO) AIMs. 'Axial' AIMs were referred to as dystonic posturing, represented by a twisting of the neck and torso directed toward the side of the body contralateral to the lesion. 'Limb' AIMs were defined as rapid, purposeless movements of the forelimb located on the side of the body contralateral to the lesion. 'Orolingual' AIMs were composed of repetitive openings and closings of the jaw and tongue protrusions and considered abnormal as they occur at times when the rats were not chewing or gnawing on food or other objects. Rats were observed for ALO AIMs for 60 sec

every 10th min over 160-200 min. A severity score of 0-4 was assigned for each AIMs category: 0, not present; 1, present for <50% of the observation period; 2, present for >50% of the observation period; 3, present for the entire observation period and interrupted by a loud stimulus (a tap on the plastic cylinder), or 4, present for the entire observation period but not interrupted by a loud stimulus. Scores for axial, limb and orolingual were combined to create a single ALO AIMs score for data analysis. The theoretical maximum ALO AIMs score was 12 per time period (4×3 AIMs subcategories) with overall maximum scores of: 192 for 160 min (12×16 time periods), 216 for 180 min (12×18 time periods), and 240 for 200 min (12×20 time periods). ALO AIMs data were analyzed using non-parametric statistics.

Drug treatments

Two weeks following lesion, 6-OHDA-lesioned rats received L-dopa methyl ester (12 mg/kg, s.c.; Sigma-Aldrich) + DL-serine 2-(2,3,4-trihydroxybenzyl) hydrazide hydrochloride (benserazide; 15 mg/kg, s.c.; Sigma-Aldrich) once per day for 7 days (days 14 to 21 post-surgery). One week following this L-dopa priming regimen (approximately 28 days post-surgery), all rats received L-dopa, followed by the 5-HT1A receptor agonist (+)-8-Hydroxy-2-(dipropylamino)tetralin hydrobromide (8-OH-DPAT; 0.2 mg/kg, s.c.; Sigma-Aldrich; 65 min post-L-dopa) and the 5-HT1A receptor antagonist, N-[2-[4-(2-Methoxyphenyl)-1-piperazinyl]ethyl]-N-2-pyridinylcyclohexanecarboxamide maleate salt (WAY100635; 0.3 mg/kg, s.c.; Sigma-Aldrich; 105 min post-L-dopa). At approximately 35 days post-surgery, dyskinetic rats, which had a total ALO AIMs score ≥ 25 on the 7th day of priming, received the D1 receptor agonist R(+)-SKF-81297 hydrobromide (SKF81297; 0.8 mg/kg, s.c.; Sigma-Aldrich), followed by 8-OH-DPAT (45 min post-SKF81297) and WAY100635 (65 min post-SKF81297). Approximately 42 days post-surgery, three of the dyskinetic rats received the D2 receptor agonist (-)-Quinpirole hydrochloride (quinpirole; 0.2 mg/kg, s.c.; Sigma-Aldrich),

followed by 8-OH-DPAT (45 min post-quinpirole) and WAY100635 (65 min post-quinpirole). The time course of behavior, surgery, electrophysiological recordings, and drug treatments are portrayed in Figure 1A.

Electrophysiological recordings

Following surgery, once per week for 4 weeks for intact control (n=4) and partially lesioned (n=4) rats and for 5-6 weeks for dyskinetic/fully-lesioned rats (n=9), spike trains and LFP activity were recorded (see Fig 1A). Each recording session for all rats included periods of rest and treadmill walking as previously described.[10] Beginning 2 weeks after surgery, treadmill walking and rest were followed by drug treatment and concomitant AIMs ratings. 6-OHDA-lesioned rats were primed with L-dopa in order to study the emergence of abnormal involuntary movements (i.e., AIMs) following loss of DA. Similarly, dyskinetic rats were later treated with D1 or D2 receptor agonists to further examine relationships between DA receptor stimulation and AIMs associated with loss of DA. At approximately 28 days post-surgery, all rats were recorded following sequential treatment of L-dopa, 8-OH-DPAT, and WAY100635 in order to compare the relationship between spiking activity and LFPs under these various conditions.

Signals from each microwire of the electrode bundle were duplicated by the preamp (Plexon, Dallas, TX) to allow differential processing by low pass filters to provide LFP channels and high-pass filters to provide waveform channels to be used for spike sorting. High-pass filtered waveform channels were amplified by 10,000×, digitized at 40 kHz, and bandpass filtered between 300 to 8,000 Hz. Low-pass filtered LFP channels were amplified by 1000×, sampled at 1 or 2 kHz, and filtered between 0.7 to 150 Hz. Single units were sorted off-line based on clustering and principal component analysis using Spike2 software (see Data analysis, below).

Histology

Rats were deeply anesthetized and recording sites were marked by electrolytic lesions. Rats were perfused intracardially with 200 ml of cold saline followed by 200 ml of 4% paraformaldehyde in phosphate-buffered saline. Fixed brains were sliced and 35 µm coronal sections containing the substantia nigra pars compacta were immunostained for tyrosine hydroxylase (TH; primary rabbit polyclonal anti-TH antibody, 1:200 dilution; Pel-Freez Biologicals; and biotinylated anti-rabbit IgG secondary antibody, 1:200 dilution; Vector Labs). The staining was processed using avidin-biotin-perioxidase complex (ABC kit; Vector Labs) and 0.05% 3,3'-diaminobenzidine tetrahydrochloride with 0.01% H_2O_2 (DAB kit; Vector Labs) until intense brown color emerged. ImageJ software (NIH) was used to evaluate the extent of TH staining for each rat (total of 3-4 sections/rat).

As expected, in intact control rats (n=4), tyrosine hydroxylase-staining of the neurons and fibers in the substantia nigra of the hemisphere that contained the electrode was not different from staining in the contralateral hemisphere (average 104±4%). In 6-OHDA-lesioned rats that developed dyskinesia (median ALO AIMs = 56±13 and 73±15 on days 1 and 7 of L-dopa priming, respectively), data showed severe loss of TH-stained neurons and fibers in the substantia nigra of the lesioned hemisphere (98±1% reduction) compared to the contralateral substantia nigra of the non-lesioned hemisphere (Fig 1B). These rats (n=9) constitute the "Full Lesion" group. Data from rats that received 6-OHDA lesions but did not become dyskinetic revealed an incomplete loss of tyrosine hydroxylase-stained neurons and fibers with an average 67±8% reduction compared to the non-lesioned hemisphere (Fig 1B). As such, these rats (n=4) are referred to as the "Partial Lesion" group. To verify electrode bundle placement, recording sites in all rats were marked by the electrolytic lesion and

sections were counterstained with cresyl violet and 5% potassium ferricyanide/9% HCl to reveal iron disposition marking the location of the electrode tips.

Data analysis

LFP and extracellular unit activity were analyzed using custom-written Spike2 and MATLAB (MathWorks) scripts. As the standard analysis of dyskinesia using the well-established AIMs scale is typically based on a 60 sec epoch,[42, 43] similar epochs were used for calculation of LFP power in the present study. Thus, epochs of 60 sec, representative of the overall periods of inattentive rest and treadmill walking that were free of major artifacts, were used to calculate LFP power. For each recording day with L-dopa priming, six epochs (60 sec each) were selected for LFP power analyses, corresponding to the onset, peak, and offset of dyskinetic behaviors. Six epochs (60 sec each) were also chosen for each recording day that included 8-OH-DPAT and WAY100635 treatments. Data for the 8-OH-DPAT and WAY100635 epochs were taken at 5 and 15 min, respectively, following drug injection. For each rat, data from at least two wires per epoch were used for power, peak and dominant frequency, and spike-triggered waveform averages (STWAs). Since rats with left hemispheric DA cell lesions experienced difficulty walking contraversive to the lesion, data were taken only when rats were walking in the ipsiversive direction in the circular treadmill.

Spectral analysis of LFPs. Power was assessed in two frequency ranges: high beta (25-35 Hz) and high gamma (70-110 Hz). Using MATLAB scripts, Fourier-transform (FFT)-based spectrograms were constructed to illustrate the evolution of spectral power during treadmill walking and rest epochs as well as over an entire recording session during L-dopa priming and drug treatments. LFP power spectral density signal-to-noise ratio was calculated as the ratio between LFP power and the 1/f-like noise spectrum (obtained by fitting the local minima of the $1/f^{\alpha}$ function, $0<\alpha<2$, to the LFP power spectrum).[40, 44, 45] These longer sets of

data were normalized with this approach in order to compensate for any extraneous/instrumental fluctuations over time and to allow for better comparisons with other studies using this approach.[40] Power was considered significant when exceeding the half power point level (~3 dB). For each 1 sec bin of recording, total power spectral density was calculated within the high beta (25-35 Hz) and high gamma (70-110 Hz) frequency bands. Dominant frequency was defined as the maximum frequency, indicated by higher total power, between high beta (25-35 Hz) and high gamma (70-110 Hz) frequency bands.

Similar to our previous studies,[9-12] shorter epochs of FFT-based power spectra (60 sec epochs of total power, as presented in the bar graphs) were obtained using a custom written Spike2 script from LFP waveforms that were smoothed to 500 Hz from their original sampling frequency (1000 or 2000 Hz). Inspection of the data showed that there was relatively little variability in the raw voltage levels over frequencies of interest within each group of rats (i.e., signals were within 3 standard deviations of the mean) and little evidence of significant extraneous/instrumental fluctuations between groups, indicating that normalization procedures were not necessary for these data sets. Peak frequencies in power spectra in the high beta range during treadmill walk epochs were identified as significant if they met three criteria. First, the peak frequency amplitudes were larger than those in the preceding and following eight 1 Hz frequency bins.[46, 47] Second, power spectrum slope changed sign from positive before the peak to negative after the peak. Third, data surrounding the maximum had a downward concavity according to second derivative analysis. Changes in power over high beta and high gamma frequency bands and peak frequency in the high beta frequency band were analyzed using two-way ANOVA and one-way and two-way repeated-measures (RM) ANOVA with post hoc comparisons with the level of significance $p<0.05$.

Cell sorting and motor cortex cell type classification. Prior to off-line spike sorting, waveforms were filtered using a digital 300 Hz high-pass filter in order to ensure complete

removal of large low frequency artifacts (Spike2; CED, Cambridge, UK). The threshold for minimum action potential amplitude for each high-pass waveform channel was designated as 3 times the root mean square (RMS) amplitude of the waveform. Spikes were then sorted using principal component analysis (PCA) together with normal mixtures clustering analysis (Spike2). As previously described,[10] well isolated cortical spikes were categorized as either putative pyramidal neurons or interneurons according to the characteristics of the spike waveform average. The trough-to-peak durations of the waveform averages were bimodally distributed and were separated into two different clusters,[10, 48] with the shorter duration group including action potential average widths in the 0.1-0.28 ms range and the longer group exceeding 0.32 ms duration. Based on the bimodal distribution of the present data, the criterion for dividing putative pyramidal spikes from interneuronal spikes was set at 0.30 ms. Only spike trains with average firing rates ≥0.2 Hz were included. The majority (291/319, 91% of recorded spike trains) had action potential durations >0.32 ms and were classified as putative pyramidal neurons. In this paper, the terms pyramidal neuron and interneuron refer to putative pyramidal and putative interneurons, respectively. Due to the relatively small number of interneurons per condition, only pyramidal neurons are represented in the analyses.

Spike-triggered waveform analysis. To assess the temporal relationship between the spiking activity of individual cortical pyramidal neurons and LFP oscillations, spike timing and phase with respect to spike-triggered waveform averages (STWAs) were quantified during 100 sec epochs. Four distinct epochs from each group (intact control, full lesion, and partial lesion) on Day 28 post-surgery were chosen for STWAs, including treadmill walking and post-L-dopa, -8-OH-DPAT, and -WAY100635 treatments. LFPs were bandpass filtered (70-110 Hz) using an FIR filter (Spike2). Peak-to-trough amplitudes of the STWAs at or around the spike (zero time) were obtained as a measure of phase locking of spike train to the

dominant LFP oscillation. Each spike train was then shuffled 10 times and each shuffled spike train was used to create an STWA. The peak-to-trough values of the shuffled STWAs were normally distributed. Spikes were considered to be significantly correlated with the LFP oscillations when the peak-to-trough amplitude of the unshuffled spike train STWA was greater than 3 standard deviations of the mean of the shuffled distribution. To assess the extent of phase locking of cortical pyramidal neurons in each group and for each epoch, mean ratios of unshuffled/shuffled peak-to-trough amplitudes for spike trains and the percentage of spike trains significantly correlated to LFP were obtained and analyzed using two-way ANOVA and chi-squared tests, respectively. For phase-locked spike trains, the phase angles between spikes and the high gamma LFP range oscillations were examined using the Rayleigh and Mardia-Watson-Wheeler tests. Unless stated otherwise, all results in this manuscript are presented as the mean value ± SEM and the significance level is alpha = 0.05.

Results

Cortical high beta (25-35 Hz) oscillatory LFP activity during treadmill walking is dependent upon degree of DA cell lesion

The current experiment included 3 groups of rats: intact control, partially DA-lesioned, and fully DA-lesioned (see Methods and Fig 1 for details). In agreement with previous data,[10, 12, 49] high beta (25-35 Hz) LFP power in the motor cortex of the lesioned hemisphere in fully-lesioned rats was significantly increased during treadmill walking compared to both intact control and partially-lesioned rats (Fig 2A, 2C and 2E). Interestingly, in fully-lesioned animals, high beta power (Fig 2B) and peak frequency (Fig 2D) were higher on day 14 post-surgery compared to day 7, which agrees with prior findings showing an

enhancement in high beta peak frequency during treadmill walking between day 7 and day 21 post-lesion.[10]

In the present experiment, fully-lesioned rats exhibited impaired stepping consistently each week for the 4 weeks post-surgery (week 1, 14±10% of the intact side steps; week 2, 13±10%; week 3, 16±13%; week 4, 17±12%; Fig 1C). In contrast, partially-lesioned rats progressively improved their stepping performance each week post-surgery (week 1, 31±14%; week 2, 49±23%; week 3, 80±17%; week 4, 87±25%). Moreover, although partially-lesioned rats demonstrated motor deficits in the stepping test at 1 and 2 weeks post-lesion compared to their pre-lesion stepping (Fig 1C), there were no significant differences in oscillatory LFP power within the high beta frequency range (25-35 Hz) in the motor cortex during treadmill walking in these partially-lesioned rats compared to intact controls (Fig 2A, 2C, and 2E). Intriguingly, partially-lesioned rats exhibited lower LFP power in the high beta range during rest on days 14 and 28 post-surgery compared to both fully-lesioned and intact control rats. Neither intact control nor partially-lesioned rats showed differences in high beta power between treadmill walking and rest; whereas fully-lesioned rats consistently showed greater high beta power during treadmill walking compared to rest (Fig 2A, 2B, 2C, and 2E).

L-dopa priming attenuates cortical high beta (25-35 Hz) LFP power and peak frequency during treadmill walking in rats with full unilateral DA cell lesions

Between days 14 and 21 post-surgery, 6-OHDA-lesioned rats received L-dopa (12 m/kg, + benserazide, 15 mg/kg, s.c.) once daily for 7 days to examine the effects of chronic L-dopa treatment (termed “L-dopa priming”; Fig 1A). Recordings of treadmill walking and rest epochs were performed on days 14 and 21 post-surgery before L-dopa injection. This allowed comparisons of LFP activity prior to L-dopa injection on day 14 with that obtained on day 21, approximately 24 hours after day 6 of L-dopa priming. Our findings reveal that L-

dopa priming dampened the expression of cortical oscillatory activity in the high beta range during treadmill walking in fully-lesioned rats (Fig 2C). Moreover, in addition to a reduction in power in the high beta range, L-dopa priming was associated with a significant reduction in the peak frequency of high beta activity during treadmill walking in fully-lesioned rats from ~32 Hz on day 14 to ~29 Hz on day 21 (Fig 2D). This reduction in the peak frequency of high beta over the week of L-dopa priming contrasts with the observation that high beta power and peak frequency increased between days 7 and 14 post-surgery (Fig 2C), before L-dopa treatment in these rats. Interestingly, on day 28 post-surgery, after a week without L-dopa treatment, these shifts towards control values in high beta power and peak frequency in fully-lesioned rats were reversed (Fig 2C, 2D, 2E).

L-dopa priming expands the durations of both the decrease in cortical high beta power and the increase in the expression of dyskinesia in rats with full unilateral DA cell lesions

On the first and last days of L-dopa priming, recordings were made that included: rest and treadmill walking before L-dopa treatment, as well as five 60 sec periods at different time points post-L-dopa administration, corresponding to onset (20 min), peak (60, 90, and 120 min), and offset (170 min) of dyskinetic behavior (Figs 3-4). These recordings showed that L-dopa priming expanded the duration of the decrease in beta power in conjunction with an acceleration of the onset and a delay of the offset of dyskinesia. High beta LFP power was significantly reduced 20 min post-L-dopa on both days 1 and 7 of priming (Fig 3A) compared to treadmill walking (prior to L-dopa). However, the decrease in high beta power was more pronounced on the last day of priming compared to the first (Fig 3A). Furthermore, on day 1 of priming, high beta power was further diminished at 60, 90, and 120 min post-L-dopa compared to the 20 min time point, whereas the decrease in power was stable at 20, 60, 90, and 120 min on the 7^{th} day of L-dopa priming. While high beta power recovered at 170 min

post-L-dopa on day 1 of priming, power was lower at this time point on the 7th day of L-dopa priming compared to the first day (Fig 3A).

These differences are relevant to the dyskinetic profile for each day. While axial, limb, and orolingual (ALO) AIMs were negatively correlated with total high beta power on the first day of L-dopa priming (Fig 3C; $r = -0.79$; $p<0.01$), as well as the last day (Fig 3D; $r = -0.38$; $p<0.05$), ALO AIMs did not develop until after 20 min on the first day of priming, whereas they were well established by this time point on the 7th day of priming (Fig 4G-H). These ALO AIMs scores are comparable to those reported in previous studies.[27, 42, 43] Taken as a whole, these data indicate that L-dopa priming is associated with a progressive decrease in high beta power in the motor cortex of dyskinetic rats and an increase in the onset and duration of L-dopa-induced dyskinesia.

Partially-lesioned rats did not develop ALO AIMs (data not shown) and there were no changes in high beta power in these rats in any behavioral state on either day of priming (Fig 3B). Similarly, L-dopa priming did not affect high beta power during treadmill walking in partially-lesioned rats (Fig 2C and 2E; Fig 3B). Furthermore, unlike the results in fully-lesioned rats (discussed below), cortical LFP power in the high gamma (70-110 Hz) range was not modified post-L-dopa in partially-lesioned rats on either day of priming (Fig 3F).

Cortical high gamma (70-110 Hz) LFP oscillatory activity is associated with the development of L-dopa-induced dyskinesia in rats with full unilateral DA cell lesions

The development of AIMs in fully-lesioned rats (Fig 4G-H) was accompanied by the emergence of high gamma LFP oscillatory activity in the motor cortex. Similar to Halje et al. (2012),[40] representative FFT-based spectrograms of LFP spectral power show the dramatic high gamma narrow band activity (with a peak ~80 Hz) that results from L-dopa treatment (Fig 4A-B). This 80 Hz activity that emerged on the first day of L-dopa priming (Fig 4A)

appears earlier and persists longer on the 7th day of priming (Fig 4B). In order to examine the relationship between high beta and high gamma activity during L-dopa priming, the total power in the high beta (25-35 Hz) and high gamma (70-110 Hz) frequency ranges for each 1 sec bin of recording was determined. Of the two frequency ranges considered, the dominant frequency, corresponding to the range with the higher total power in that bin, was plotted (Fig 4C-D). The fluctuations in dominant frequency (as determined by greater total power) between high beta and high gamma were greater on the first day of priming (Fig 4C) compared to the last day (Fig 4D), suggesting that cortical high gamma activity is more stable by the end of L-dopa priming. In addition, cortical high gamma LFP power showed an earlier onset, a longer duration, and was more intense on the 7th day of priming compared to the first (Fig 4E-F). On the 7th day of priming, high gamma power was significantly increased at 20, 60, 90, and 120 min post-L-dopa compared to treadmill walking epochs, whereas high gamma power was significantly increased at only 90 and 120 min post-L-dopa on the first day of priming (Fig 3E). High gamma power on the last day of priming was also greater during peak dyskinesia time periods (60, 90, and 120 min post-L-dopa) compared to the early 20 min period. Furthermore, day 7 of priming revealed greater high gamma power compared to day 1 at 20, 60, 90, and 120 min post-L-dopa. Collectively, these findings demonstrate a positive correlation between the development of ALO AIMs behavior and cortical high gamma LFP power, which is evident on the first (Fig 3G; $r = 0.41$; $p<0.01$) and last (Fig 3H; $r = 0.36$; $p<0.05$) day of L-dopa priming.

Changes in cortical high beta and high gamma power during L-dopa priming are likely independent phenomena

While it may be tempting to argue that the differences in high beta and high gamma power during L-dopa priming reflect interactions leading to an inverse relationship between

the two frequency ranges (i.e., as the level of high beta power decreases, high gamma power increases), our data do not fully support this concept. High gamma power was additionally enhanced between the first and last day of priming at peak dyskinesia time periods (i.e. 60, 90 and 120 min; Fig 3A), while high beta power was not further diminished. It is however likely that high beta power was not further diminished due to a floor effect.

While both high beta and high gamma power are negatively and positively correlated with total ALO AIMs scores, respectively (Fig. 3C-D, 3G-H; Table 1), these relationships become less clear upon closer examination. Although high gamma LFP power was significantly enhanced at 90 and 120 min post-L-dopa on the first day of priming (Fig 3E), average ALO AIMs developed much earlier (30 min post-L-dopa; Fig 4G). On the 7th day of priming, high gamma power was greater at time points 60, 90, and 120 min post-L-dopa compared to 20 min post-L-dopa (Fig 3E) but ALO AIMs were not similarly enhanced (Fig 4H). However, this lack of an increase in ALO AIMs scores could be explained by a ceiling effect and limitation of the AIMs scale. Moreover, on the last day of priming at 170 min post-L-dopa, ALO AIMs were still present (Fig 4H) despite a lack of significantly enhanced high gamma power (Fig 3E). As shown in Figure 4E-F, high gamma power became significantly enhanced at approximately 50 min on day 1 of priming and 20 min on day 7, while ALO AIMs emerged sooner at 30 min and 10 min on days 1 and 7, respectively. High beta power re-emerged, while high gamma power diminished, between 140 and 160 min on day 1 (Fig 4E) and at approximately 170 min on day 7 (Fig 4F), though ALO AIMs were still present during these times (Fig 4G-H). These inconsistencies in the time courses of exaggerated cortical high gamma LFP activity and dyskinesia raise questions about the functional relationship between the two phenomena.

There are also differences observed between the specific AIMs subtypes. The ALO AIMs scale is comprised of 3 abnormal behaviors including: axial, limb, and orolingual (see

Methods). Axial, limb, and orolingual AIMs were each negatively correlated with high beta total LFP power on both days 1 and 7 of priming, though each AIMs subcategory was significantly less correlated on the last day compared to the first (see Table 1). Interestingly, axial AIMs were not significantly correlated with high gamma power on either day 1 or 7 of L-dopa priming, limb AIMs were correlated equally on both days, and orolingual AIMs were correlated on day 1 but not day 7. Thus, whereas cortical high beta power is highly negatively correlated with all types of AIMs, the positive correlation between cortical high gamma LFP power and AIMs depends on the type of dyskinetic behavior that is being displayed. The association of increased high gamma power with some dyskinetic movements, but not others, is a possible route to better understanding the functional significance of high gamma power in movement.

D1 and D2 receptor agonists independently induce dyskinesia and cortical high gamma oscillations

In order to further explore the relationship between cortical high gamma LFP activity and dyskinesia, we investigated the ability of DA receptor agonists to induce dyskinesia 2-3 weeks following L-dopa priming (see Fig 1A). Similar to previous research,[23-25] systemic administration of both D1 and D2 receptor agonists independently induced ALO AIMs (Fig 5D and 5F) that were similar to L-dopa-induced AIMs (Fig 5B). Notably, both agonists significantly enhanced cortical high gamma power (Fig 5C-5F, 5H, and 5I) similar to levels that were induced by L-dopa (Fig 5A-B, 5G).

5-HT1A receptor stimulation reduces cortical high gamma oscillations

One week following the end of the L-dopa priming period (day 28 post-surgery; Fig 1A), L-dopa (12 mg/kg, s.c. + benserazide, 15 mg/kg, s.c.) administration once again induced

a significant enhancement of cortical high gamma LFP oscillatory activity and concomitantly induced ALO AIMs expression in fully-lesioned rats (Fig 5A-B). Similar to the effects seen during priming at these time points, there was greater total high gamma power, and less high beta power, at 60, 120, and 170 min post-L-dopa compared to treadmill walking (Fig 5G). Strikingly, the 5-HT1A receptor agonist 8-OH-DPAT (0.2 mg/kg, s.c.; injected 85 min post-L-dopa) dramatically and rapidly reduced L-dopa-induced increases in cortical high gamma LFP power (Fig 5A, 5B, 5G) and, similar to previous reports,[24, 50] also reduced ALO AIMs (Fig 5B). 8-OH-DPAT restored high beta power to levels observed during treadmill walking (Fig 5G). Although rats were in the open cylinder and not walking on the treadmill during this time period, they were behaviorally alert and attentive. Beta levels during these epochs were similar to those in our recent report of increased high beta power in the substantia nigra pars reticulata during alert non-walking states in hemiparkinsonian rats.[11] Subsequent 5-HT1A receptor antagonist WAY100635 (0.3 mg/kg, s.c.; injected 105 post-L-dopa) administration restored the L-dopa-induced effects on high gamma power, high beta power, and ALO AIMs (Fig 5A, 5B, 5G).

As described in the previous section, administration of the D1 receptor agonist SKF81297 (day 35 post-surgery) and the D2 receptor agonist quinpirole (day 42 post-surgery; Fig 1A) induced ALO AIMs expression while significantly increasing cortical high gamma LFP power (Fig 5C-F). Furthermore, SKF81297 induced decreases in high beta power at 20, 40, 50, 80, and 120 min post-injection compared to epochs of treadmill walking in fully-lesioned rats (Fig 5H). Administration of 8-OH-DPAT (0.2 mg/kg, s.c.; injected 45 min post-SKF81297) led to a rapid reduction in cortical high gamma LFP power relative to that observed at 20 and 40 min post-SKF81297 (Fig 5C, 5D, and 5H). However, this reduction in high gamma power was more modest than that induced by 8-OH-DPAT in the L-dopa treated rats, and high gamma power remained significantly greater post-8-OH-DPAT

compared to levels during treadmill walking (Fig 5H). This effect was associated with increased rotational activity that is distinct from ALO AIMs[51] and often observed with this treatment combination.[24, 52] Furthermore, 8-OH-DPAT did not reverse SKF81297-induced decreases in high beta power in contrast to its effects when administered after L-dopa. Moreover, in contrast to its moderate reduction of high gamma power, and in agreement with previous reports,[24, 52] 8-OH-DPAT dramatically reduced SKF81297-induced ALO AIMs (Fig 5D). Subsequent treatment with WAY100635 (0.3 mg/kg, s.c.; injected 65 post-SKF81297) reversed 8-OH-DPAT's effects on cortical high gamma LFP power and ALO AIMs.

Similar to results with L-dopa and SKF81297, quinpirole increased high gamma power, while decreasing high beta power, at 20, 40, 80, and 170 min post-injection compared to treadmill walking (Fig 5I). Following 8-OH-DPAT (0.2 mg/kg, s.c.; injected 45 min post-quinpirole), cortical high gamma LFP power was significantly reduced and high beta power was significantly increased compared to 20 and 40 min post-quinpirole (Fig 5E, 5F, and 5I). Although 8-OH-DPAT increased high beta power more after quinpirole compared to after SKF81297, high beta power was still lower compared to treadmill walking (Fig 5I). As with L-dopa and SKF81297, 8-OH-DPAT administration led to a reduction in quinpirole-induced ALO AIMs (Fig 5F). Rats were behaviorally alert and attentive with little to no rotational activity, similar to a previous report using this treatment combination.[24] Subsequent administration of WAY100635 (0.3 mg.kg, s.c.; injected 65 min post-quinpirole) reversed these neuronal and behavioral effects (Fig 5E, 5F, 5I).

Collectively, these findings indicate that stimulating inhibitory 5-HT1A receptors decreases high gamma LFP activity while at the same time reducing dyskinesia induced by L-dopa and DA agonists. However, subtle differences in drug effects on high gamma power as compared to AIMs expression raise questions about the extent of this correlation over the series of drug treatments.

Cortical spiking activity and LFPs are significantly phase locked in the high gamma range but phase locking decreases as LFP power increases

Finally, we examined the relationship between cortical spiking and LFPs in the high gamma range (70-110 Hz) during recordings that included treadmill walking followed by sequential treatment with L-dopa, 8-OH-DPAT, and WAY100635 in our 3 groups of rats (fully-lesioned, partially-lesioned, and intact control rats) at approximately day 28 post-surgery (Fig 1A). Cortical spike trains were categorized as either putative pyramidal neurons or interneurons based on average action potential duration, and due to the limited number of interneurons (28/319, 9% of recorded spike trains), the findings reported here represent exclusively pyramidal neurons.

Interestingly, STWAs revealed significant robust spike-LFP phase locking in the high gamma range (70-110 Hz) in all groups in each behavioral state (i.e., treadmill walking, post-L-dopa, post-8-OH-DPAT, and post-WAY100635; Fig 6B). Unexpectedly, spike-LFP phase locking during L-dopa-induced dyskinesia was reduced compared to treadmill walking in fully-lesioned rats (Fig 6B-C). When 8-OH-DPAT was administered to these dyskinetic rats, ALO AIMs were reduced (Fig 5B) in conjunction with a reversal of the L-dopa-induced decrease in spike-LFP phase locking (Fig 6B-C). Subsequent WAY100635 administration restored both L-dopa-induced ALO AIMs (Fig 5B) and L-dopa-induced decreases in phase locking (Fig 6B-C). These findings demonstrate that spike-LFP phase locking decreased (Fig 6B-C) when high gamma LFP power increased (Fig 5G). In fact, significant negative correlations between spike-LFP phase locking and high gamma power were found in all 3 groups of rats (Fig 6D-F).

This counterintuitive inverse relationship between the spiking activity of cortical pyramidal neurons and high gamma LFP power led to further analyses, including the phase-

locking of spikes to LFPs from other wires from the same bundle of electrodes in the motor cortex in the 70-110 Hz range. Analyses revealed that there were no significant differences in ratios or percentages of correlated spikes between treadmill walking and L-dopa-induced dyskinesia in fully-lesioned rats when using the LFP waveforms recorded from other wires in the bundle (1.7 ratio and 25% correlated vs. 1.8 ratio and 29%, respectively). If spike timing was positively influenced by fluctuations in high gamma LFP power, there would be greater STWA ratios and a higher percentage of correlated spikes during L-dopa-induced dyskinesia (enhanced high gamma power) relative to treadmill walking (minimal high gamma power), regardless of the wire used. These results support the initial findings of a downward trend of spike-LFP phase locking from treadmill walking to L-dopa-induced dyskinesia in fully-lesioned rats (Fig 6B-C).

In addition to measures of the degree of spike-LFP phase locking, the phase angles between spikes from phase-locked spike trains and the high gamma range LFP oscillations were examined. For each group of rats, spikes in the majority of the motor cortex pyramidal spike trains were significantly oriented with respect to their own LFP oscillations, filtered between 70 to 110 Hz, in each behavioral condition. Mean preferred phase angles ranged from 159 to 168 degrees for the intact group, 176 to 183 degrees for the partially-lesioned group, and 174 to 180 degrees for the fully-lesioned group, depending on the behavior (Fig 6D). Mean phase angles did not vary significantly within each group with respect to changes in LFP power. There was, however, a trend for the phases of the intact group to occur slightly earlier than those in the lesioned groups, but this was only significant in the WAY condition, where cortical spiking in the intact group occurred ~0.48 and ~0.40 ms sooner compared to those in the partially-lesioned and fully-lesioned groups, respectively.

Discussion

The present study used the unilateral 6-OHDA rat model to explore the functional significance of cortical high gamma LFP oscillations in PD during dyskinesia and their impact on high beta range activity. Results are reported from three distinct groups: fully DA-lesioned, partially DA-lesioned, and intact control rats. Our findings show that L-dopa priming attenuates the cortical high beta activity that is associated with parkinsonian bradykinesia in the fully-lesioned rats[9-12] and promotes the emergence of a relatively narrow band of high gamma LFP activity (70-110 Hz range with a peak frequency ~80 Hz) in the motor cortex in conjunction with L-dopa-induced dyskinesia. Furthermore, high gamma LFP activity increased in power and L-dopa-induced dyskinesia increased in duration between the first and last day of L-dopa priming in fully-lesioned rats. These observations are consistent with recent studies showing high gamma activity in the motor cortex and striatum of rats with L-dopa-induced dyskinesia[12, 40] and may be relevant to clinical reports of FTG activity in the motor cortex, globus pallidus internal segment (GPi), subthalamic nucleus (STN), and thalamus in PD patients following DA replacement therapy.[37-39, 53-56] Although the direct pathway has been more highly implicated in the mechanisms underlying L-dopa-induced dyskinesia than the indirect pathway,[33-36] we show that both D1 and D2 receptor agonists independently induced both the 80 Hz cortical high gamma oscillations and dyskinetic behaviors in the L-dopa primed rat. Furthermore, the anti-dyskinetic 5-HT1A receptor agonist 8-OH-DPAT reduced both high gamma and dyskinesia, while the 5-HT1A receptor antagonist WAY100635 reversed these effects. While our data point to a possible functional correlation between narrow band high gamma cortical activity and dyskinesia, closer examination of the relationships between each AIMs behavior, cortical spiking, and high gamma LFP power raises doubts about the extent of this correlation, as discussed below.

Activity in both beta and high gamma frequency ranges in various nuclei of the basal ganglia-thalamocortical circuit have been observed in PD patients and experimental animal

models of PD. Though the specific beta frequency ranges vary between species, with higher frequencies (25-40 Hz) in the rat[8-12] and lower frequencies (8-30 Hz) in humans and monkeys,[1, 3-7, 13-17, 46] it is generally hypothesized that exaggerated beta oscillations may contribute to motor impairment in the parkinsonian condition. In the present experiment, rats with full, unilateral DA cell lesions showing both impaired stepping and exaggerated high beta (25-35 Hz) LFP activity in the lesioned hemisphere of the motor cortex during treadmill walking also showed small but significant increases in peak beta frequency over time post lesion. Interestingly, the increases in peak frequency in the high beta range observed here between days 7 and 14 post-lesion are consistent with previous studies showing that the peak frequency of LFP power in the high beta range incrementally increases from day 7 to days 21 and 40-50 post DA cell lesion,[10, 11] supporting the idea of gradually emerging plasticity following DA cell loss.

Moreover, the lack of exaggerated cortical high beta activity during treadmill walking in the rats with partial lesions (67±8% nigral TH loss) in the current experiment is consistent with recent findings showing that rats with partial lesions via 6-OHDA injections into the medial forebrain bundle or through intracerebroventricular administration (72% and 65% depletion, respectively) do not show exaggerated beta activity in the substantia nigra pars reticulata during treadmill walking.[49] Notably, partially-lesioned rats in the present study showed significant motor deficits in the stepping test during the first and second weeks post-lesion and then showed improvement during the third and fourth week post-lesion. Collectively, these results support the suggestion that the increase in beta band activity arises in late-stage, severely DA-depleted conditions and that exaggerated increases in beta power may not be causative, but rather compensatory, maladaptive, and/or epiphenomenal, of the motor impairments associated with loss of DA in the basal ganglia-thalamocortical circuit[6, 49, 57-60]

L-dopa treatment has been shown to reduce these exaggerated beta range LFP activities in the cortex, GPi, and STN in human PD patients.[5, 61-64] In addition, therapeutic doses of L-dopa (4-5 mg/kg) have been shown to decrease high beta LFP activity in the motor cortex and substantia nigra pars reticulata of the lesioned hemisphere in rats with unilateral DA cell loss of at least 90%.[9, 10] The current study provides further insight into acute and chronic effects of L-dopa administration on cortical high beta activity in fully-lesioned rats. Relative to the effects of acute L-dopa on the first day of priming, chronic administration of L-dopa was associated with a more rapid onset of the reduction in beta power and induction of dyskinesia, indicating a sensitization of response of both phenomena. Chronic L-dopa treatment also led to reductions in cortical high beta power and peak frequency during treadmill walking. Interestingly, cortical high beta LFP power and peak frequency during treadmill walking were restored to pre-priming levels following one week without L-dopa treatment, suggesting that the decreases in high beta power and peak frequency were contingent upon continuous DA replacement therapy. Collectively, previous research[10] and the present study show that L-dopa reduces cortical power in the beta range in severely DA-depleted conditions, regardless of whether the dose of L-dopa is therapeutic or dyskinesia-inducing. Given that the partially-lesioned rats in the current experiment did not show exaggerated high beta activity during treadmill walking, it was not surprising that L-dopa treatment did not affect high beta power in these rats.

In addition to reductions in high beta activity, L-dopa treatment has been shown to induce an increase in high gamma activity in a narrow band between 60-90 Hz, referred to as "finely-tuned gamma" (FTG),[39] in the motor cortex, GPi, STN, and thalamus in PD patients[37, 38, 54-56, 64-66] and in the motor cortex and striatum in rodent models of PD.[12, 40] In the current experiment, sustained cortical high gamma oscillations (70-110 Hz with a peak frequency ~80 Hz) emerged in conjunction with dyskinetic behavior induced by L-dopa treatment

in fully-lesioned rats. The partially-lesioned rats failed to show significant increases in narrow band high gamma activity or dyskinesia during L-dopa priming, suggesting that the emergence of L-dopa-induced narrow band high gamma activity in the hemiparkinsonian rat depends upon DA lesion severity. The relatively more powerful emergence of the band on the 7th day of L-dopa priming compared to the first day in the fully-lesioned rats, as well as the positive correlations between total high gamma LFP power and ALO AIMS on both days of priming, support the idea of a positive relationship between the two phenomena. However, it is important to note that axial AIMs were not correlated with high gamma power on either day of L-dopa priming, forelimb AIMs were positively correlated equivalently on each day of priming, and orolingual AIMs were positively correlated on the first day of priming but not the last.

In an effort to better understand this relationship between cortical narrow band high gamma LFP activity and dyskinesia, pharmacological agents known to induce or decrease dyskinesia were utilized following L-dopa priming. Systemic administration of the D1 agonist SKF81297 and the D2 agonist quinpirole independently elicited exaggerated cortical high gamma LFP activity and dyskinesia. These findings expand upon previous work showing the importance of the D1 receptor in generating high gamma oscillations during L-dopa-induced dyskinesia[40] with novel data showing the involvement of stimulation of the D2 receptor in eliciting this rhythm in conjunction with dyskinesia. Interestingly, while administration of the 5-HT1A receptor agonist 8-OH-DPAT similarly reduced L-dopa- and DA agonist-induced ALO AIMs, high gamma LFP power was diminished by varying degrees. These results demonstrate that changes in high gamma power occur in conjunction with changes in dyskinesia but raise questions about the extent of this correlation over the series of drug treatments.

Further support for a disconnect between narrow band high gamma activity and dyskinesia may come from clinical recordings in the motor cortex, thalamus, GPi, and STN.[37, 38, 54, 55] The expression of FTG is not unique to PD patients receiving L-dopa as it has also been observed in patients with essential tremor, dystonia, and epilepsy.[54, 67, 68] Although we did not observe it in the motor cortex of our intact control or partially-lesioned rats following L-dopa, increased high gamma activity (~80 Hz) has been reported in the ventral striatum of healthy rodents following DA agonist treatment with both apomorphine and amphetamine.[69] In addition, transient and focal bursts of high gamma (60-100 Hz) activity have been reported in the sensorimotor and primary motor cortices of healthy human participants during motor tasks.[70-73] FTG is also often lateralized in healthy participants,[74] dystonic patients,[75] and patients with essential tremor,[68] occurring just prior to and during movement. Thus, while the functional correlate to FTG remains uncertain, there is evidence that FTG is associated with arousal and that high gamma power increases along with increases in the speed or amount of movement.[39, 64, 68]

A number of studies have shown that neuronal spiking activity tends to be phase-locked to exaggerated beta range LFP activity in the basal ganglia of PD patients, supporting the view that under certain conditions, LFP can be used as a surrogate for synchronized spiking activity.[4, 6, 7, 55] However, in the current experiment, spike-LFP phase locking and cortical high gamma LFP power was negatively correlated. Studies exploring the mechanisms underlying the expression of gamma range activity in the cortex have pointed to the participation of local subcircuits generating recurrent rhythms via interactions between pyramidal neurons and inhibitory interneurons, referred to as pyramidal-interneuronal gamma (PING).[76-79] However, the expectation that increased power would be associated with increased phase locking of pyramidal neurons in the motor cortex (layers 5/6) in the current study is not supported by the data. Another potential mechanism suggests that cortical gamma

reflects subthreshold LFP oscillations driven by upstream input, such as the thalamus.[39, 77] Indeed, preliminary findings from our lab show that administration of the $GABA_A$ agonist muscimol into the ventromedial thalamus prior to L-dopa (Brazhnik et al., SfN abstract 2013) or 90 min post-L-dopa (Dupre et al., SfN abstract 2015) eliminates cortical high gamma LFP activity without modifying dyskinesia scores. These findings support the idea that subcortical input may be contributing to this narrow range gamma, as proposed for FTG,[2, 39] while also supporting the possibility of a dissociation between cortical high gamma and dyskinesia.

A causative relationship between high gamma LFP power and dyskinesia remains to be definitively demonstrated. Here we have utilized a well-established model of dyskinesia to explore the development of narrow band high gamma activity in the motor cortex of hemiparkinsonian rats. Though methodological differences exist, the narrow band high gamma activity reported here is seemingly similar to FTG observed in clinical reports and its apparent association with dyskinesia in the rat model suggests it could provide insight into processes contributing to dyskinesia in the PD patient. A major advantage of using the rodent model to explore this phenomenon is that we are able to perform chronic recordings over time in various behavioral states in one or more nuclei at a time, obtaining simultaneously both LFP and neuronal spiking activity. In the present study, we have shown that narrow band high gamma activity appears positively correlated with L-dopa-induced dyskinesia under several conditions but we have also found evidence for some inconsistencies in this relationship. Current studies are underway to explore other nuclei of the basal ganglia-thalamocortical circuit during L-dopa-induced dyskinesia in order to better understand the relationship between this high gamma rhythm and dyskinesia.

References

1. Brown P. Oscillatory nature of human basal ganglia activity: Relationship to the pathophysiology of Parkinson's disease. Movement disorders : official journal of the Movement Disorder Society 2003;18(4):357-363.
2. Brittain JS, Brown P. Oscillations and the basal ganglia: motor control and beyond. Neuroimage 2014;2:637-647.
3. Brown P, Oliviero, A., Mazzone, P., Insola, A., Tonali, P., Di Lazzaro, V. Dopamine dependency of oscillations between subthalamic nucleus and pallidum in Parkinson's disease. The Journal of neuroscience : the official journal of the Society for Neuroscience 2001;21(3):1033-1038.
4. Levy R, Ashby, P., Hutchison, W.D., Lang, A.E., Lozano, A.M., Dostrovsky, J.O. Dependence of subthalamic nucleus oscillations on movement and dopamine in Parkinson's disease. Brain 2002;125:1196-1209.
5. Priori A, Foffani G, Pesenti A, et al. Rhythm-specific pharmacological modulation of subthalamic activity in Parkinson's disease. Exp Neurol 2004;189(2):369-379.
6. Weinberger M, Mahant N, Hutchison WD, et al. Beta oscillatory activity in the subthalamic nucleus and its relation to dopaminergic response in Parkinson's disease. Journal of neurophysiology 2006;96(6):3248-3256.
7. Kuhn AA, Trottenberg T, Kivi A, Kupsch A, Schneider GH, Brown P. The relationship between local field potential and neuronal discharge in the subthalamic nucleus of patients with Parkinson's disease. Exp Neurol 2005;194(1):212-220.
8. Sharott A, Magill PJ, Harnack D, Kupsch A, Meissner W, Brown P. Dopamine depletion increases the power and coherence of beta-oscillations in the cerebral cortex and subthalamic nucleus of the awake rat. The European journal of neuroscience 2005;21(5):1413-1422.
9. Avila I, Parr-Brownlie LC, Brazhnik E, Castaneda E, Bergstrom DA, Walters JR. Beta frequency synchronization in basal ganglia output during rest and walk in a hemiparkinsonian rat. Exp Neurol 2010;221(2):307-319.
10. Brazhnik E, Cruz AV, Avila I, et al. State-dependent spike and local field synchronization between motor cortex and substantia nigra in hemiparkinsonian rats. The Journal of neuroscience : the official journal of the Society for Neuroscience 2012;32(23):7869-7880.
11. Brazhnik E, Novikov N, McCoy AJ, Cruz AV, Walters JR. Functional correlates of exaggerated oscillatory activity in basal ganglia output in hemiparkinsonian rats. Exp Neurol 2014;261:563-577.
12. Delaville C, McCoy AJ, Gerber CM, Cruz AV, Walters JR. Subthalamic nucleus activity in the awake hemiparkinsonian rat: relationships with motor and cognitive networks. The Journal of neuroscience : the official journal of the Society for Neuroscience 2015;35(17):6918-6930.
13. Bergman H, Wichmann T, Karmon B, DeLong MR. The primate subthalamic nucleus. II. Neuronal activity in the MPTP model of parkinsonism. Journal of neurophysiology 1994;72(2):507-520.
14. Gatev P, Darbin O, Wichmann T. Oscillations in the basal ganglia under normal conditions and in movement disorders. Movement disorders : official journal of the Movement Disorder Society 2006;21(10):1566-1577.
15. Devergnas A, Pittard D, Bliwise D, Wichmann T. Relationship between oscillatory activity in the cortico-basal ganglia network and parkinsonism in MPTP-treated monkeys. Neurobiology of disease 2014;68:156-166.

16. Raz A, Vaadia E, Bergman H. Firing patterns and correlations of spontaneous discharge of pallidal neurons in the normal and the tremulous 1-methyl-4-phenyl-1,2,3,6-tetrahydropyridine vervet model of parkinsonism. The Journal of neuroscience : the official journal of the Society for Neuroscience 2000;20(22):8559-8571.
17. Rivlin-Etzion M, Elias S, Heimer G, Bergman H. Computational physiology of the basal ganglia in Parkinson's disease. Prog Brain Res 2010;183:259-273.
18. Jankovic J. Motor fluctuations and dyskinesias in Parkinson's disease: clinical manifestations. Movement disorders : official journal of the Movement Disorder Society 2005;20 Suppl 11:S11-16.
19. Chondrogiorgi M, Tatsioni A, Reichmann H, Konitsiotis S. Dopamine agonist monotherapy in Parkinson's disease and potential risk factors for dyskinesia: a meta-analysis of levodopa-controlled trials. Eur J Neurol 2014;21(3):433-440.
20. Stathis P, Konitsiotis, S., Antonini, A. Dopamine agonists early monotherapy for the delay of development of levodopa-induced dyskinesias. Expert Rev Neurother 2015;15(2):207-213.
21. Rascol O, Brooks, D.J., Korczyn, A.D., De Deyn, P.P., Clarke, C.E., Lang, A.E. A five-year study of the incidence of dyskinesia in patients with early Parkinson's disease who were treated with ropinirole or levodopa. N Engl J Med 2000;342(20):1484-1491.
22. Rascol O, Nutt, J.G., Blin, O., Goetz, C.G., Trugman, J.M., Soubrouillard, C., Carter, J.H., Currie, L.J., Fabre, N., Thalamas, C., Giardina, W.J., Wright, S. Induction by dopamine D1 receptor agonist ABT-431 of dyskinesia similar to levodopa in patients with Parkinson's disease. Arch Neurol 2001;58:249-254.
23. Drake JD, Kibuuka LN, Dimitrov KD, Pollack AE. Abnormal involuntary movement (AIM) expression following D2 dopamine agonist challenge is determined by the nature of prior dopamine receptor stimulation (priming) in 6-hydroxydopamine lesioned rats. Pharmacol Biochem Behav 2013;105:26-33.
24. Dupre KB, Eskow KL, Negron G, Bishop C. The differential effects of 5-HT(1A) receptor stimulation on dopamine receptor-mediated abnormal involuntary movements and rotations in the primed hemiparkinsonian rat. Brain Res 2007;1158:135-143.
25. Lindenbach D, Dupre KB, Eskow Jaunarajs KL, Ostock CY, Goldenberg AA, Bishop C. Effects of 5-HT1A receptor stimulation on striatal and cortical M1 pERK induction by L-DOPA and a D1 receptor agonist in a rat model of Parkinson's disease. Brain Res 2013;1537:327-339.
26. Calon F, Rajput, A.H., Hornykiewicz, O., Bedard, P.J., Di Paolo, T. Levodopa-induced motor complications are associated with alterations of glutamate receptors in Parkinson's disease. Neurobiology of disease 2003;14:404-416.
27. Dupre KB, Ostock CY, Eskow Jaunarajs KL, et al. Local modulation of striatal glutamate efflux by serotonin 1A receptor stimulation in dyskinetic, hemiparkinsonian rats. Exp Neurol 2011;229(2):288-299.
28. Robelet S, Melon C, Guillet B, Salin P, Kerkerian-Le Goff L. Chronic L-DOPA treatment increases extracellular glutamate levels and GLT1 expression in the basal ganglia in a rat model of Parkinson's disease. The European journal of neuroscience 2004;20(5):1255-1266.
29. Sgambato-Faure V, Cenci MA. Glutamatergic mechanisms in the dyskinesias induced by pharmacological dopamine replacement and deep brain stimulation for the treatment of Parkinson's disease. Prog Neurobiol 2012;96(1):69-86.
30. Carta M, Lindgren HS, Lundblad M, Stancampiano R, Fadda F, Cenci MA. Role of striatal L-DOPA in the production of dyskinesia in 6-hydroxydopamine lesioned rats. J Neurochem 2006;96(6):1718-1727.

31. Cenci MA, Ohlin, K.E., Rylander, D. Plastic effects of L-DOPA treatment in the basal ganglia and their relevance to the development of dyskinesia. Parkinsonism Relat Disord 2009;1553:S59-S63.
32. Cenci MA. Dopamine dysregulation of movement control in L-DOPA-induced dyskinesia. Trends Neurosci 2007;30(5):236-243.
33. Darmopil S, Martin AB, De Diego IR, Ares S, Moratalla R. Genetic inactivation of dopamine D1 but not D2 receptors inhibits L-DOPA-induced dyskinesia and histone activation. Biol Psychiatry 2009;66(6):603-613.
34. Fieblinger T, Sebastianutto I, Alcacer C, et al. Mechanisms of dopamine D1 receptor-mediated ERK1/2 activation in the parkinsonian striatum and their modulation by metabotropic glutamate receptor type 5. The Journal of neuroscience : the official journal of the Society for Neuroscience 2014;34(13):4728-4740.
35. Mela F, Marti M, Bido S, Cenci MA, Morari M. In vivo evidence for a differential contribution of striatal and nigral D1 and D2 receptors to L-DOPA induced dyskinesia and the accompanying surge of nigral amino acid levels. Neurobiology of disease 2012;45(1):573-582.
36. Westin JE, Vercammen L, Strome EM, Konradi C, Cenci MA. Spatiotemporal pattern of striatal ERK1/2 phosphorylation in a rat model of L-DOPA-induced dyskinesia and the role of dopamine D1 receptors. Biol Psychiatry 2007;62(7):800-810.
37. Litvak V, Eusebio A, Jha A, et al. Movement-related changes in local and long-range synchronization in Parkinson's disease revealed by simultaneous magnetoencephalography and intracranial recordings. The Journal of neuroscience : the official journal of the Society for Neuroscience 2012;32(31):10541-10553.
38. Lopez-Azcarate J, Tainta M, Rodriguez-Oroz MC, et al. Coupling between beta and high-frequency activity in the human subthalamic nucleus may be a pathophysiological mechanism in Parkinson's disease. The Journal of neuroscience : the official journal of the Society for Neuroscience 2010;30(19):6667-6677.
39. Jenkinson N, Kuhn AA, Brown P. gamma oscillations in the human basal ganglia. Exp Neurol 2013;245:72-76.
40. Halje P, Tamte M, Richter U, Mohammed M, Cenci MA, Petersson P. Levodopa-induced dyskinesia is strongly associated with resonant cortical oscillations. The Journal of neuroscience : the official journal of the Society for Neuroscience 2012;32(47):16541-16551.
41. Olsson M, Nikkhah G, Bentlage C, Bjorklund A. Forelimb Akinesia in the Rat Parkinson Model - Differential-Effects of Dopamine Agonists and Nigral Transplants as Assessed by a New Stepping Test. Journal of Neuroscience 1995;15(5):3863-3875.
42. Cenci MA, Lundblad M. Ratings of L-DOPA-induced dyskinesia in the unilateral 6-OHDA lesion model of Parkinson's disease in rats and mice. Current protocols in neuroscience / editorial board, Jacqueline N Crawley [et al] 2007;Chapter 9:Unit 9.25.
43. Lundblad M, Andersson M, Winkler C, Kirik D, Wierup N, Cenci MA. Pharmacological validation of behavioural measures of akinesia and dyskinesia in a rat model of Parkinson's disease. The European journal of neuroscience 2002;15(1):120-132.
44. Allegrini P, Menicucci D, Bedini R, et al. Spontaneous brain activity as a source of ideal 1/f noise. Phys Rev E Stat Nonlin Soft Matter Phys 2009;80(6 Pt 1):18.
45. Palva JM, Zhigalov A, Hirvonen J, Korhonen O, Linkenkaer-Hansen K, Palva S. Neuronal long-range temporal correlations and avalanche dynamics are correlated with behavioral scaling laws. Proc Natl Acad Sci U S A 2013;110(9):3585-3590.
46. Alonso-Frech F, Zamarbide I, Alegre M, et al. Slow oscillatory activity and levodopa-induced dyskinesias in Parkinson's disease. Brain 2006;129(Pt 7):1748-1757.

47. Doyle LM, Kuhn AA, Hariz M, Kupsch A, Schneider GH, Brown P. Levodopa-induced modulation of subthalamic beta oscillations during self-paced movements in patients with Parkinson's disease. The European journal of neuroscience 2005;21(5):1403-1412.
48. Pelled G, Bergstrom DA, Tierney PL, et al. Ipsilateral cortical fMRI responses after peripheral nerve damage in rats reflect increased interneuron activity. Proc Natl Acad Sci U S A 2009;106(33):14114-14119.
49. Quiroga-Varela A, Walters JR, Brazhnik E, Marin C, Obeso JA. What basal ganglia changes underlie the parkinsonian state? The significance of neuronal oscillatory activity. Neurobiology of disease 2013;58:242-248.
50. Mignon L, Wolf WA. Postsynaptic 5-HT1A receptor stimulation increases motor activity in the 6-hydroxydopamine-lesioned rat: implications for treating Parkinson's disease. Psychopharmacology 2007;192(1):49-59.
51. Breger LS, Dunnett SB, Lane EL. Comparison of rating scales used to evaluate L-DOPA-induced dyskinesia in the 6-OHDA lesioned rat. Neurobiology of disease 2013;50:142-150.
52. Dupre KB, Ostock CY, George JA, Eskow Jaunarajs KL, Hueston CM, Bishop C. Effects of 5-HT1A receptor stimulation on D1 receptor agonist-induced striatonigral activity and dyskinesia in hemiparkinsonian rats. ACS Chem Neurosci 2013;4(5):747-760.
53. Alegre M, Alonso-Frech F, Rodriguez-Oroz MC, et al. Movement-related changes in oscillatory activity in the human subthalamic nucleus: ipsilateral vs. contralateral movements. The European journal of neuroscience 2005;22(9):2315-2324.
54. Kempf F, Brucke C, Salih F, et al. Gamma activity and reactivity in human thalamic local field potentials. The European journal of neuroscience 2009;29(5):943-953.
55. Trottenberg T, Fogelson N, Kuhn AA, et al. Subthalamic gamma activity in patients with Parkinson's disease. Exp Neurol 2006;200(1):56-65.
56. Alegre M, Lopez-Azcarate J, Alonso-Frech F, et al. Subthalamic activity during diphasic dyskinesias in Parkinson's disease. Movement disorders : official journal of the Movement Disorder Society 2012;27(9):1178-1181.
57. Degos B, Deniau JM, Chavez M, Maurice N. Chronic but not acute dopaminergic transmission interruption promotes a progressive increase in cortical beta frequency synchronization: relationships to vigilance state and akinesia. Cereb Cortex 2009;19(7):1616-1630.
58. Leblois A, Meissner W, Bioulac B, Gross CE, Hansel D, Boraud T. Late emergence of synchronized oscillatory activity in the pallidum during progressive Parkinsonism. The European journal of neuroscience 2007;26(6):1701-1713.
59. Mallet N, Pogosyan A, Sharott A, et al. Disrupted dopamine transmission and the emergence of exaggerated beta oscillations in subthalamic nucleus and cerebral cortex. The Journal of neuroscience : the official journal of the Society for Neuroscience 2008;28(18):4795-4806.
60. Syed EC, Benazzouz A, Taillade M, et al. Oscillatory entrainment of subthalamic nucleus neurons and behavioural consequences in rodents and primates. The European journal of neuroscience 2012;36(9):3246-3257.
61. Marceglia S, Foffani G, Bianchi AM, et al. Dopamine-dependent non-linear correlation between subthalamic rhythms in Parkinson's disease. J Physiol 2006;571(Pt 3):579-591.
62. Ray NJ, Jenkinson N, Wang S, et al. Local field potential beta activity in the subthalamic nucleus of patients with Parkinson's disease is associated with improvements in bradykinesia after dopamine and deep brain stimulation. Exp Neurol 2008;213(1):108-113.
63. Williams D, Tijssen, M., van Bruggen, G., Bosch, A., Insola, A., Di Lazzaro, V., Mazzone, P., Oliviero, A., Quartarone, A., Speelman, H., Brown, P. . Dopamine-dependent

changes in the functional connectivity between basal ganglia and cerebral cortex in humans. Brain 2002;125:1558-1569.
64. Tan H, Pogosyan A, Anzak A, et al. Complementary roles of different oscillatory activities in the subthalamic nucleus in coding motor effort in Parkinsonism. Exp Neurol 2013;248:187-195.
65. Devos D, Szurhaj W, Reyns N, et al. Predominance of the contralateral movement-related activity in the subthalamo-cortical loop. Clin Neurophysiol 2006;117(10):2315-2327.
66. Ozkurt TE, Butz M, Homburger M, et al. High frequency oscillations in the subthalamic nucleus: a neurophysiological marker of the motor state in Parkinson's disease. Exp Neurol 2011;229(2):324-331.
67. Pfurtscheller G, Graimann B, Huggins JE, Levine SP, Schuh LA. Spatiotemporal patterns of beta desynchronization and gamma synchronization in corticographic data during self-paced movement. Clinical Neurophysiology 2003;114(7):1226-1236.
68. Brucke C, Bock A, Huebl J, et al. Thalamic gamma oscillations correlate with reaction time in a Go/noGo task in patients with essential tremor. Neuroimage 2013;75:36-45.
69. Berke JD. Fast oscillations in cortical-striatal networks switch frequency following rewarding events and stimulant drugs. The European journal of neuroscience 2009;30(5):848-859.
70. Ball T, Demandt E, Mutschler I, et al. Movement related activity in the high gamma range of the human EEG. Neuroimage 2008;41(2):302-310.
71. Cheyne D, Bells S, Ferrari P, Gaetz W, Bostan AC. Self-paced movements induce high-frequency gamma oscillations in primary motor cortex. Neuroimage 2008;42(1):332-342.
72. Muthukumaraswamy SD. Functional properties of human primary motor cortex gamma oscillations. Journal of neurophysiology 2010;104(5):2873-2885.
73. Cheyne D, Ferrari P. MEG studies of motor cortex gamma oscillations: evidence for a gamma "fingerprint" in the brain? Front Hum Neurosci 2013;7(575).
74. Androulidakis AG, Doyle LM, Yarrow K, Litvak V, Gilbertson TP, Brown P. Anticipatory changes in beta synchrony in the human corticospinal system and associated improvements in task performance. The European journal of neuroscience 2007;25(12):3758-3765.
75. Brucke C, Kempf F, Kupsch A, et al. Movement-related synchronization of gamma activity is lateralized in patients with dystonia. The European journal of neuroscience 2008;27(9):2322-2329.
76. Borgers C, Epstein S, Kopell NJ. Background gamma rhythmicity and attention in cortical local circuits: a computational study. Proc Natl Acad Sci U S A 2005;102(19):7002-7007.
77. Lee S, Jones SR. Distinguishing mechanisms of gamma frequency oscillations in human current source signals using a computational model of a laminar neocortical network. Front Hum Neurosci 2013;7:869.
78. Whittington MA, Traub, R.D., Kopell., N., Ermentrout, B., Buhl, E.H. Inhibition-based rhythms: experimental and mathematical observations on network dynamics. Int J Psychophysiol 2000;38:315-336.
79. Whittington MA, Cunningham MO, LeBeau FE, Racca C, Traub RD. Multiple origins of the cortical gamma rhythm. Dev Neurobiol 2011;71(1):92-106.

Figure Legends

Figure 1. (A) Schematic outline of the time course for the experiment. Prior to and following surgery for unilateral electrode implantation into the left motor cortex alone (n=4) or in conjunction with unilateral 6-OHDA lesion of the medial forebrain bundle (n=13) (empty arrow), rats were trained to walk in a circular treadmill and the stepping test was performed. Following surgery, rats were recorded for treadmill walking and rest epochs (long black arrows). 6-OHDA-lesioned rats were also recorded following L-dopa treatment on the first and last days of priming in conjunction with abnormal involuntary movements (AIMs) ratings. At approximately 28 days post-surgery, following treadmill walk/rest epochs, all rats were recorded during sequential treatment of L-dopa, the 5-HT1A receptor agonist 8-OH-DPAT (DPAT), and the 5-HT1A receptor antagonist WAY100635 (WAY), and dyskinetic rats were scored for AIMs. During recordings at approximately 35 and 42 days post-surgery, dyskinetic rats (later termed "Full Lesion") received the D1 receptor agonist SKF81297 and the D2 receptor agonist quinpirole, respectively, followed by DPAT and WAY and were scored for AIMs. **(B)** Three experimental groups were confirmed upon tyrosine hydroxylase immunostaining in the substantia nigra: Intact controls (n=4; 104±4% compared to contralateral hemisphere); dyskinetic rats with full unilateral 6-OHDA-lesions (n=9; 98±1% nigral TH loss), and non-dyskinetic, partially-lesioned rats (n=4; 67±8% nigral TH loss). Relevant anatomical structures: Aq, aqueduct (Sylvius); SN, substantia nigra. **(C)** Line graph shows motor performance on the stepping test expressed as mean percentages of intact forepaw adjusting steps ± SEM for 6-OHDA-lesioned rats. While partially-lesioned rats showed initial deficit in the stepping test, their stepping progressively improved each week post-surgery. Conversely, fully-lesioned rats exhibited impaired stepping consistently each week for 4 weeks post-surgery. *Significant difference from pre-lesion. +Significance difference between full and partial lesion groups.

Figure 2. Motor cortex LFP power comparisons of intact, partially-lesioned, and fully-lesioned rats during rest and treadmill walking. **(A)** Representative FFT-based spectrograms depict time-frequency spectral power of motor cortex LFP during epochs of rest and treadmill walking on day 14 post-surgery. Spectral power was plotted with greater power being represented by red colors. Note the activity in the high beta (25-35 Hz) frequency oscillations in the fully-lesioned rats during treadmill walking, whereas a modest, more diffuse band is present in the 40-50 Hz range in intact and partially-lesioned rats during treadmill walking. Bar graphs represent mean total high beta LFP power in the motor cortex in intact control (gray; n=4), partially-lesioned (green; n=4), and fully-lesioned (red; n=9) rats during epochs of **(B)** rest and **(C)** treadmill walking on days 7, 14, 21, and 28 post-surgery. Days 7 and 14 post-surgery recordings were performed prior to any L-dopa treatment. The recording on Day 21 was 24 h after the last L-dopa (12 mg/kg + benserazide, 15 mg/kg, s.c.) treatment with 6 days of daily prior treatment. The recording on Day 28 took place one week following L-dopa priming, where the 6-OHDA-lesioned rats did not receive any L-dopa administration between days 21 and 28 post-surgery. **(D)** Mean frequency of the significant peaks in the motor cortex in fully-lesioned rats on days 7, 14, 21, and 28 post-surgery. **(E)** Linear graphs show averaged LFP power spectra for the same rest and treadmill walking epochs shown in **(B)** and **(C)**. Note that LFP power and peak frequency in the high beta range (25-35 Hz) increased between days 7 and 14 post-surgery in the fully-lesioned rats and was reduced on day 21 post-surgery, 24 h after the last L-dopa treatment (consisting of 6 days of daily treatment; i.e., L-dopa priming). L-dopa's effects on LFP power and peak frequency in the high beta range during treadmill walking in fully-lesioned rats were reversed following one

week without any L-dopa administration, as shown on day 28. *Significant difference from intact controls. +Significant difference from partially-lesioned rats. ^Significant difference from fully-lesioned rats. #Significant difference from day 7 post-surgery.

Figure 3. Total LFP power in the high beta (25-35 Hz) and high gamma (70-110 Hz) ranges over the course of L-dopa priming in fully- and partially-lesioned rats. Two weeks following surgery, fully-lesioned (n=9) and partially-lesioned (n=4) rats were injected daily with L-dopa for 7 days. Recordings were performed on the first and last days of L-dopa priming. On each day, prior to L-dopa treatment, periods of rest and circular treadmill walking were also recorded. Fully-lesioned rats developed axial, forelimb, and orolingual (ALO) AIMs. Bar graphs represent mean total LFP power in the motor cortex in the **(A)-(B)** high beta (25-35 Hz in blue) and **(E)-(F)** high gamma (70-110 Hz in red) frequency ranges in **(A, E)** fully-lesioned and **(B, F)** partially-lesioned rats on the first (lighter colors) and last (darker colors) days of L-dopa priming. Comparisons of the following 60 sec epochs were made: rest, treadmill walking, and five time periods post-L-dopa administration, corresponding to onset (20 min), peak (60, 90, and 120 min), and offset (170 min) of dyskinetic behaviors in fully-lesioned rats. Note that there were no changes in high beta and high gamma total LFP power in partially-lesioned rats that did not become dyskinetic. However, high beta power decreased while high gamma power increased in fully-lesioned rats, where the respective decreases and increases were greater on the 7^{th} day of L-dopa priming compared to the first day. Correlations between ALO AIMs scores and total power in the **(C)-(D)** high beta (in blue) and **(G)-(H)** high gamma (in red) frequency ranges during the aforementioned epochs on **(C, G)** day 1 (lighter colors) and **(D, H)** day 7 (darker colors) of L-dopa priming in fully-lesioned rats. Note that total high beta power and ALO AIMs were significantly negatively correlated, while total high gamma power and ALO AIMs were significantly positively correlated, on each day. Intriguingly, these correlations were reduced between the first and last day of priming. *Significant difference between days 1 and 7 of L-dopa priming. +Significant difference from treadmill walking. ^Significant difference from 20 min post-L-dopa.

Figure 4. LFP activity in the high beta (25-35 Hz) and high gamma (70-110 Hz) ranges over the course of L-dopa priming in fully-lesioned rats. Two weeks following surgery, fully-lesioned rats (n=9) were injected daily with L-dopa for 7 days. Recordings were performed on the **(A, C, E, G)** first and **(B, D, F, H)** last days of L-dopa priming. **(A)-(B)** Representative FFT-based spectrograms depict time-frequency spectral power of motor cortex LFP during L-dopa priming. LFP power spectral density signal-to-noise ratio (SNR) was calculated as the ratio between LFP power and the fitted 1/f-like noise spectrum. Spectral power was plotted as a SNR (dB) with greater power being represented by red colors. **(C)-(D)** Representative diagrams of the dominant frequency between 25-35 Hz (in blue) and 70-110 Hz (in red) following L-dopa administration during priming. For each 1 sec bin of recording, total spectral power was calculated as the average power in a frequency range defined as the maximum frequency ±3 Hz within the high beta (25-35 Hz) and high gamma (70-110 Hz) frequency bands. Dominant frequency was defined as the frequency with higher total power between high beta and high gamma frequency bands. **(E)-(F)** Average LFP total power (25-35 Hz in blue and 70-110 Hz in red), where darker colored areas represent significant power. Power was considered significant when exceeding the half power point level (~3 dB). **(G)-(H)** Median axial, forelimb, and orolingual (ALO) AIMs (± median absolute deviation) every 10 min post-L-dopa for each day. These ALO AIMs data are also overlaid onto the dominant frequency and power plots in **(C)-(F)**. Note that expressions of high gamma oscillatory activity and dyskinetic behavior occurred earlier, persisted longer, and were more robust on

the 7th day of priming compared to the first. *Significant difference between days 1 and 7 of L-dopa priming.

Figure 5. The effects of 5-HT1A receptor agonist administration on L-dopa- and dopamine (DA) agonist-mediated high gamma LFP activity and dyskinesia. One to three weeks following the end of L-dopa priming, fully-lesioned rats were recorded for periods of rest and circular treadmill walking, followed by administration of: **(A, B, G)** L-dopa (12 mg/kg + benserazide, 15 mg/kg, s.c.; n=9), **(C, D, H)** the D1 receptor agonist SKF81297 (0.8 mg/kg, s.c.; n=9), and **(E, F, I)** the D2 receptor agonist quinpirole (0.2 mg/kg, s.c.; n=3). During peak dyskinesia (85 min post-L-dopa or 45 min post-DA agonists), rats were injected with the 5-HT1A receptor agonist 8-OH-DPAT (0.2 mg/kg, s.c.), followed 20 min later by the 5-HT1A receptor antagonist WAY100635 (0.3 mg/kg, s.c.). **(A, C, E)** Representative FFT-based spectrograms depict time-frequency spectral power of motor cortex LFP during treatments. Spectral power was plotted as a signal-to-noise ratio (dB) with greater power being represented by red colors. **(B, D, F)** Lines depict average LFP total power (±SEM in pink) in the high gamma (70-110 Hz) range (in red) on the left axis, and median axial, forelimb, and orolingual (ALO) AIMs (± median absolute deviation) score (in black) on the right axis. **(G, H, I)** Bar graphs represent mean total LFP power in the motor cortex in the high beta (25-35 Hz; in light gray) and high gamma (70-110 Hz; in dark gray) frequency ranges in fully-lesioned rats that received the aforementioned treatments. Comparisons were made of the following 60 sec epochs: rest, treadmill walking, and six time periods post-L-dopa or DA agonist administration, consisting of time periods that normally include onset, peak, and offset of dyskinetic behaviors. 8-OH-DPAT was administered during peak dyskinesia time periods (epochs were chosen 5 min post-8-OH-DPAT), followed twenty minutes later by WAY100635 (epochs were chosen 15 min post-WAY100635). Note that 8-OH-DPAT reduced high gamma LFP power and ALO AIMs, regardless of whether dyskinesia was induced by L-dopa, SKF81297, or quinpirole. Interestingly, however, 8-OH-DPAT induced an increase in high beta LFP power in only the L-dopa and quinpirole treated rats. Importantly, WAY100635 reversed all of these effects. *Significant difference from 8-OH-DPAT (90 min post-L-dopa or 50 min post-DA agonist). +Significant difference from treadmill walking.

Figure 6. Analysis of spike-LFP relationships in the high gamma (70-110 Hz) frequency range in the motor cortex of intact control, partially-lesion, and fully-lesioned rats. At approximately 28 days post-surgery, all rats were recorded for circular treadmill walking and rest epochs, followed by sequential treatment with L-dopa (12 mg/kg, s.c. + benserazide, 15 mg/kg, s.c.) + the 5-HT1A receptor agonist 8-OH-DPAT (DPAT; 0.2 mg/kg, s.c.) + the 5-HT1A receptor antagonist WAY100635 (WAY; 0.3 mg/kg, s.c.). **(A)** Representative spike-triggered waveform averages (STWAs) of a pyramidal neuron in layers 5/6 of the motor cortex of a fully-lesioned rat during: treadmill walking, 60 min post-L-dopa, 5 min post-8-OHDPAT (90 min post-L-dopa), and 15 min post-WAY100635 (120 min post-L-dopa). **(B)** Bars show mean ratios of peak-trough amplitudes of the original ("unshuffled") STWA relative to the mean of 10 shuffled STWAs for LFPs in the 70-110 Hz range for putative cortical pyramidal neurons. Each bar represents the mean ratio of STWA amplitudes and **(C)** percentage of correlated spike trains (firing rate > 0.2 Hz) in a 100 sec behavioral epoch (treadmill walk, 60 min post-L-dopa, 5 min post-DPAT, and 15 min post-WAY) for intact control (in gray; n=4), partially-lesioned/non-dyskinetic (in green; n=3), and fully-lesioned/dyskinetic (in red; n=9) rats. Note that STWA ratios and the percentage of significantly correlated spike trains in the fully-lesioned rats are decreased 60 min post-L-dopa, increase after 8-OH-DPAT, and decrease again following WAY100635. Conversely,

high gamma LFP power and dyskinesia increase following L-dopa, decrease after 8-OH-DPAT, and increase again after WAY100635 (see Fig 5A, 5B, 5G). **(D)** Phase plots showing the distributions of phase relationships between cortical spikes and cortical LFPs filtered between 70 and 110 Hz for spike trains showing significant phase locking to local LFP in all 3 groups of rats during each behavioral epoch. Spikes were significantly oriented to high gamma cortical LFP oscillations in all cases (Rayleigh test, all $p<0.05$). Arrows reflect the strength of concentration of the distribution of the mean phase values, normalized to the radius of the circular plot. Correlations between total high gamma (70-110 Hz) LFP power and STWA ratios in **(E)** intact controls (in gray), **(F)** partially-lesioned rats (in green), and **(G)** fully-lesioned rats (in red). Note that LFP total power in the high gamma range (70-110 Hz) is negatively correlated with STWA ratios, demonstrating that phase locking of cortical spike-LFP decreases as high gamma power increases. While all groups show this negative correlation, fully-lesioned rats become dyskinetic and exhibit much greater high gamma power. *Significant difference from treadmill walking. +Significant difference from 8-OH-DPAT. #Significant difference from intact control.

Figure 1

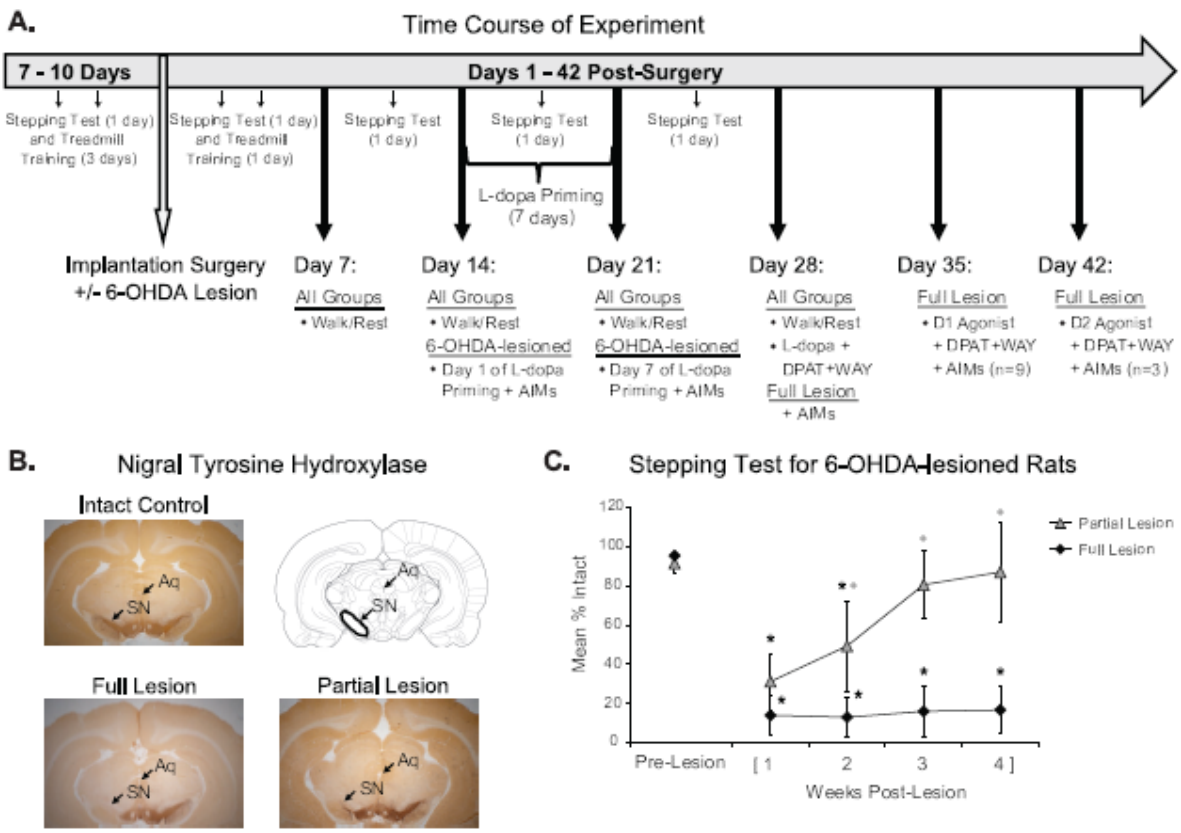

Figure 2

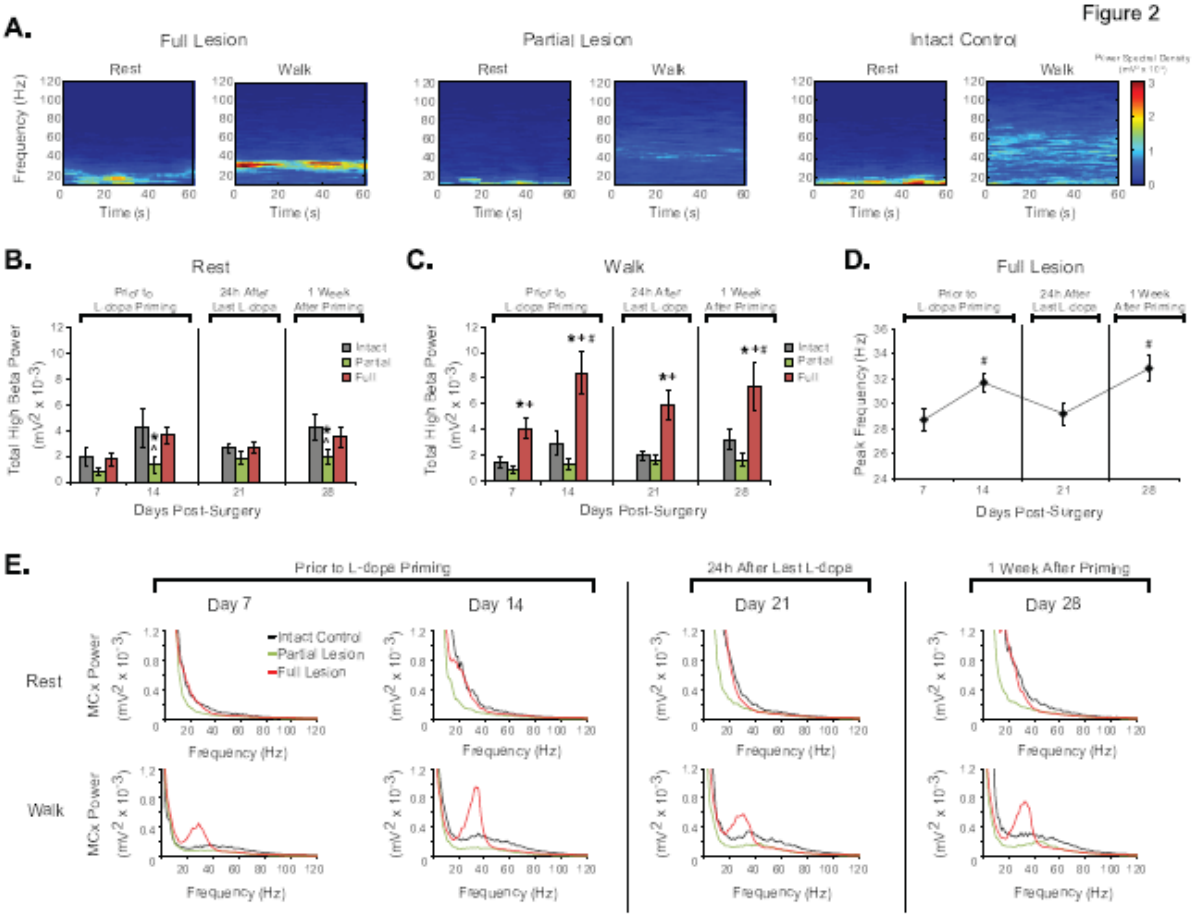

Figure

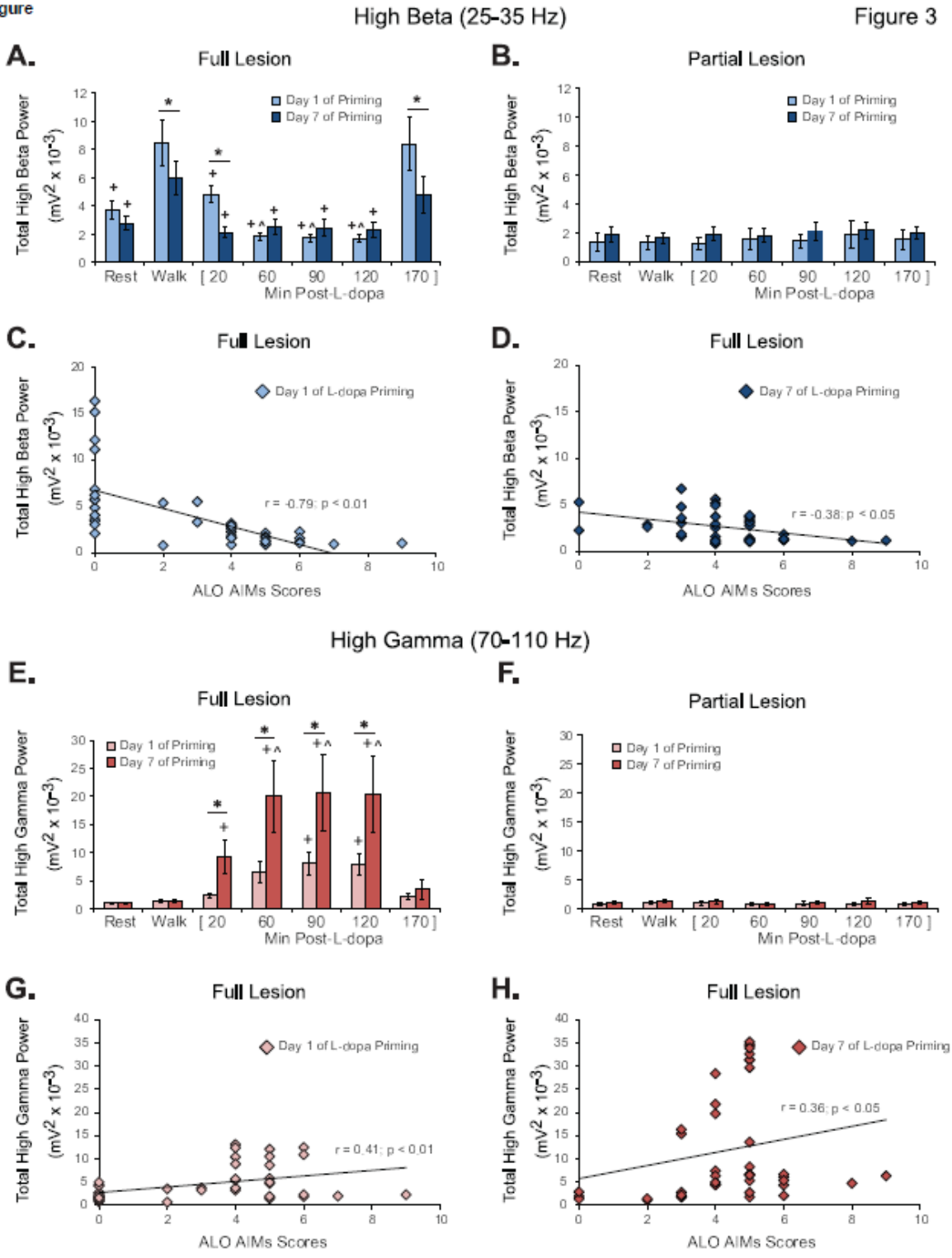

Figure 3

Figure 4

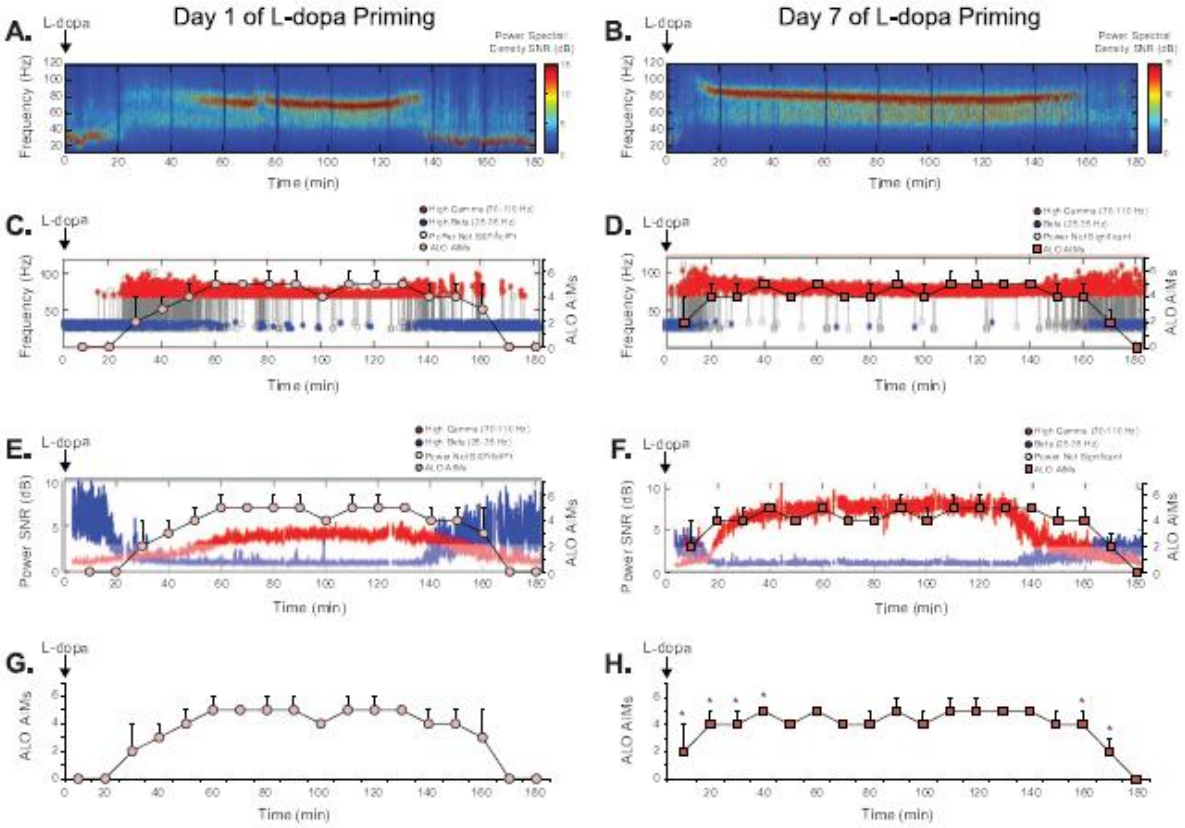

Figure 5

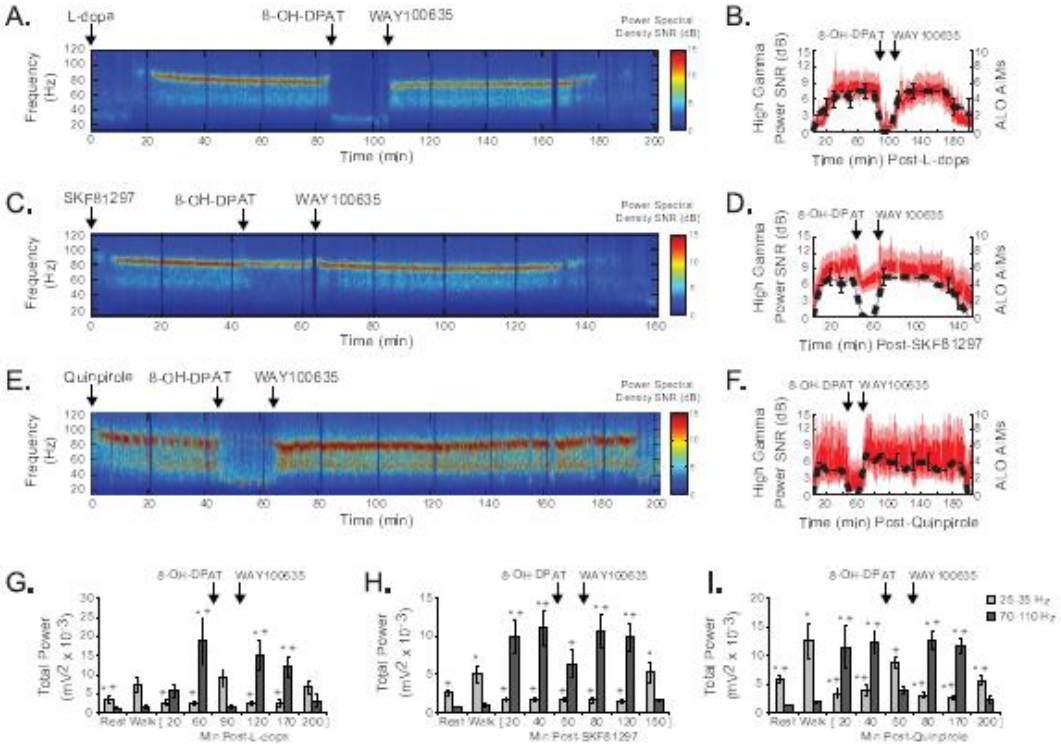

Figure 6

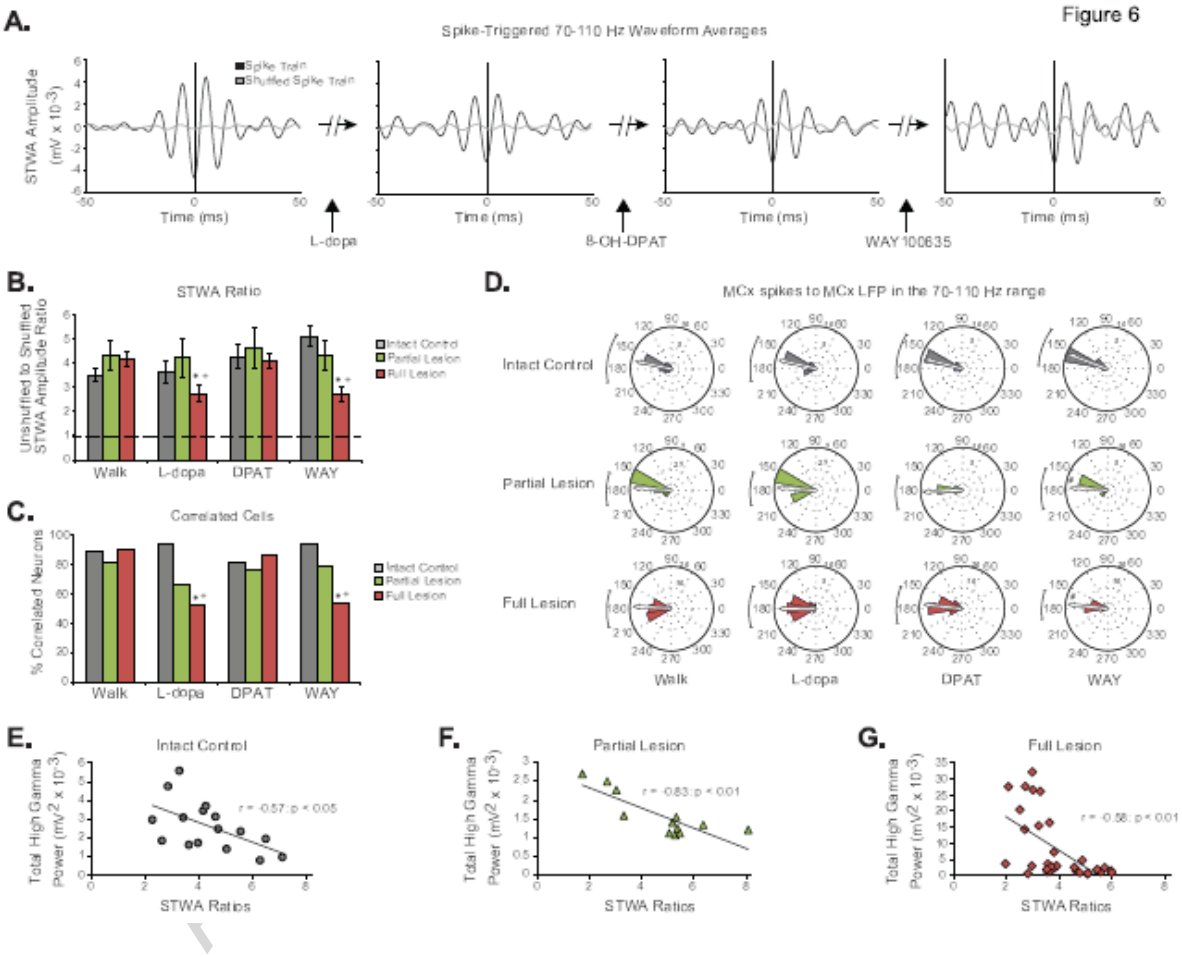

Table 1. Spearman's rank correlation coefficients between power in the high beta (25-35 Hz) and high gamma (70-110 Hz) frequency ranges and abnormal involuntary movements (AIMs), including the total AIMs and its subcategories:
Axial, Limb, and Orolingual, on the first and last days of L-dopa priming in fully-lesioned rats.

ALO AIMs	High Beta (25-35 Hz) Power		High Gamma (70-110 Hz) Power	
	Priming Day 1	Priming Day 7	Priming Day 1	Priming Day 7
Total	-0.79**	-0.38*+	0.41**	0.36*
Axial	-0.76**	-0.36*+	0.27	0.14
Limb	-0.80**	-0.36*+	0.43**	0.45**
Orolingual	-0.69**	-0.53**	0.37*	0.21

* p <0.05; ** p<0.01; + p<0.05 vs. Priming Day 1